

LS Scienza dei Materiali - a.a. 2008/09

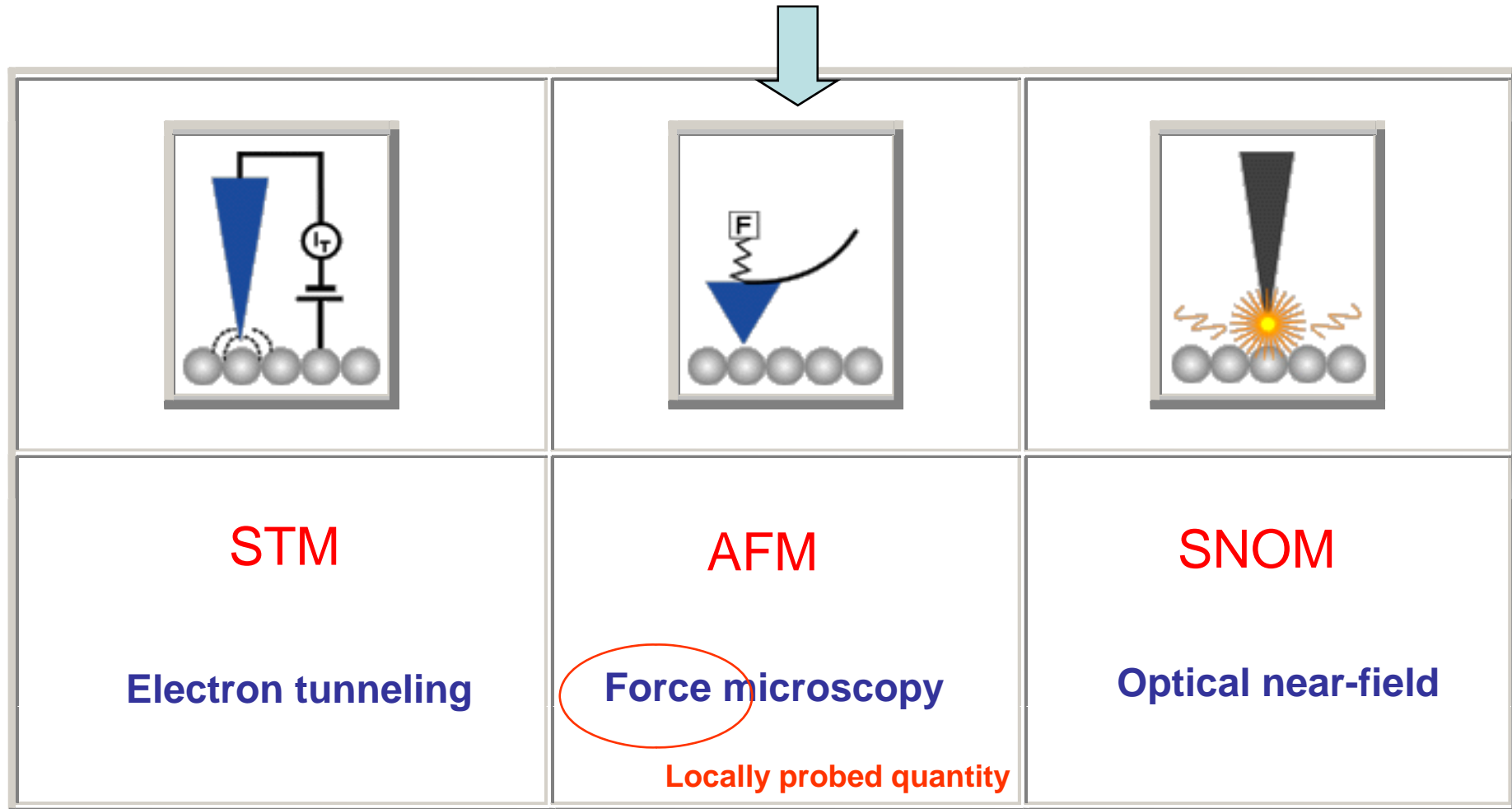
Fisica delle Nanotecnologie – part 5.2

Version 7, Nov 2008

Francesco Fuso, tel 0502214305, 0502214293 - fuso@df.unipi.it
<http://www.df.unipi.it/~fuso/dida>

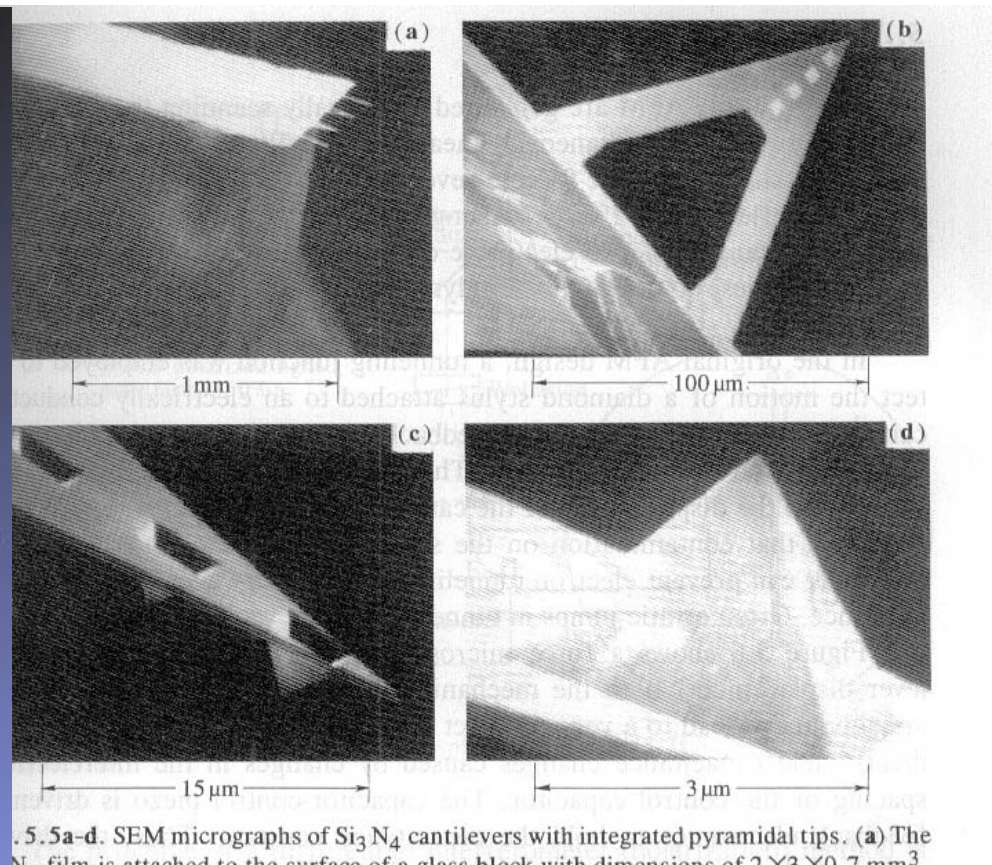
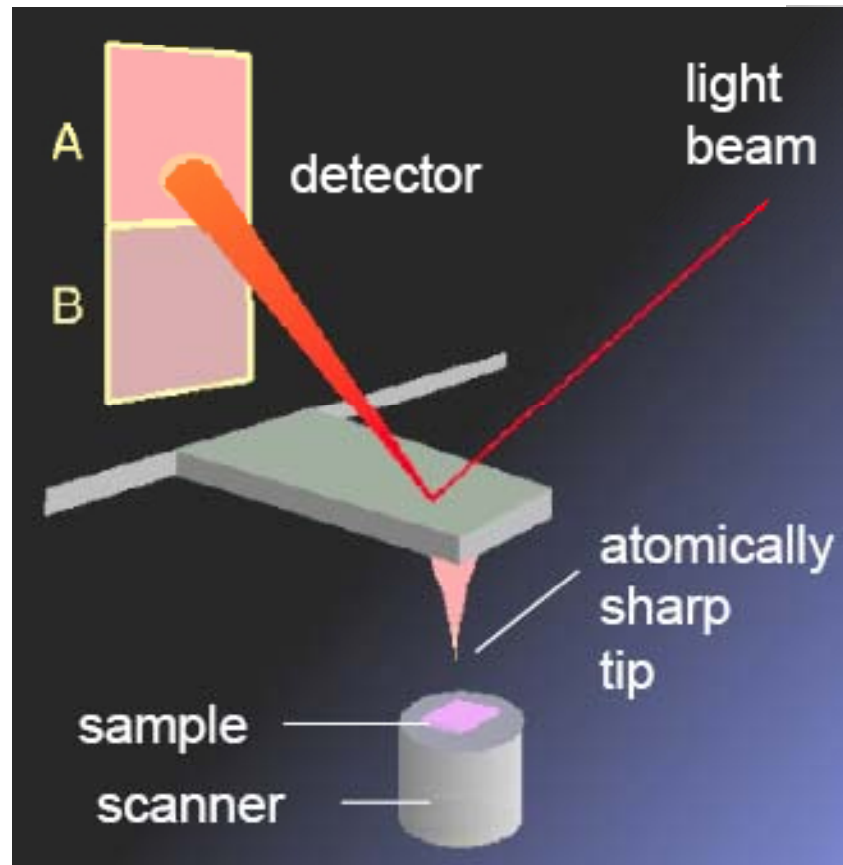
Tecniche a scansione di sonda per nanoscopia e nanomanipolazione 2: AFM e derivati

2. Scanning force microscopy (AFM and relatives)



AFM is probably the most straightforward (and easy to understand/interpret) probe microscopy

AFM probes



5.5a-d. SEM micrographs of Si_3N_4 cantilevers with integrated pyramidal tips. (a) The Si_3N_4 film is attached to the surface of a glass block with dimensions of $2 \times 3 \times 0.7 \text{ mm}^3$. Four cantilevers protrude from the edge of the block. (b) Four pyramidal tips can be seen at the end of this V-shaped cantilever. (c) The pyramidal tips are hollow when viewed from the back side. (d) Each tip has very smooth sidewalls, and the tip appears to terminate virtually at a point, with less than 30 nm radius [5.4]

The local character of AFM relies on the availability of suitable probes

Cantilever/tip fabrication: examples

The first step in the fabrication of an AFM tip is the etching of a single-crystal silicon wafer with specific crystalline orientation. This results in the forming of square pyramidal tips with characteristic angles.

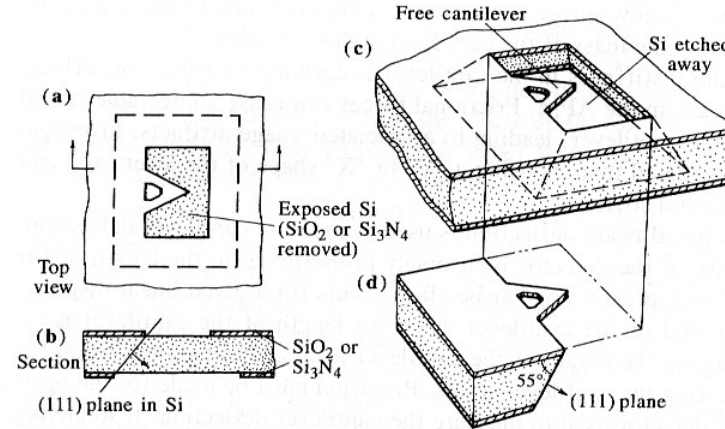
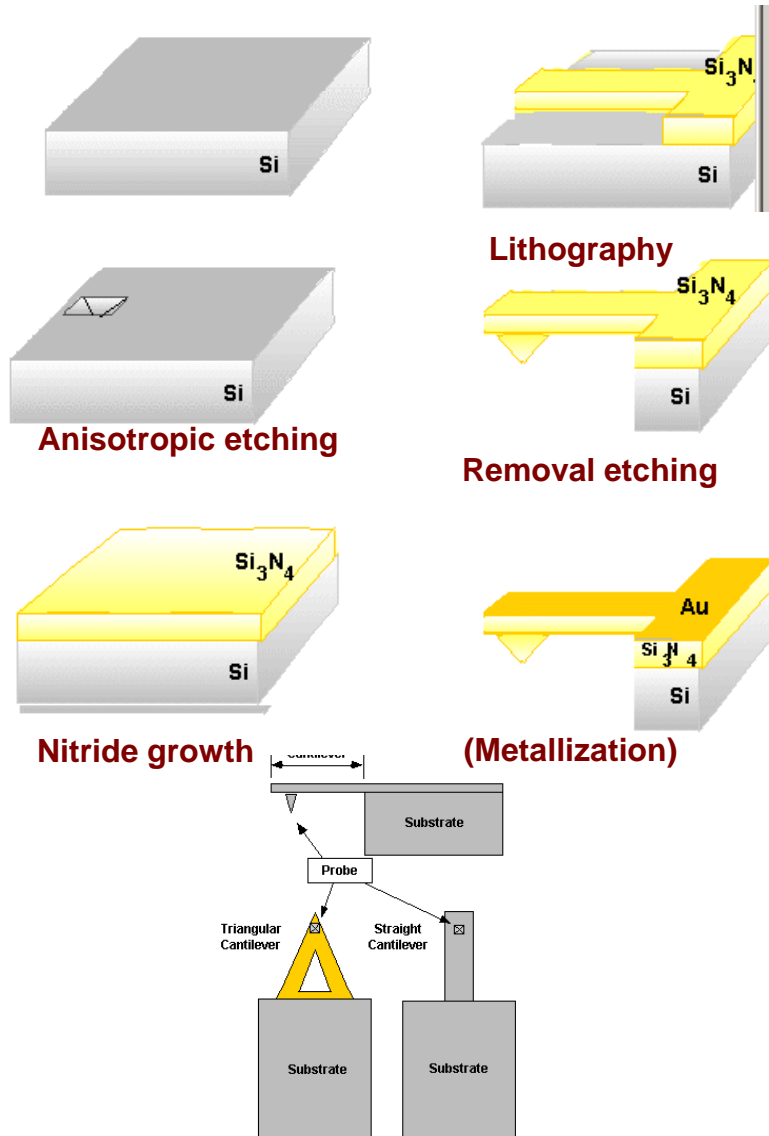


Fig. 5.2a-d. Fabrication of thin-film microcantilevers. (a) A thin film of SiO_2 or Si_3N_4 is formed on the surface of a (100) Si wafer and patterned to define the shape of the cantilever and to create openings on the top and bottom of the wafer. (b) The windows are aligned along (111) planes. (c) Anisotropic etching of the exposed Si with KOH undercuts the cantilever and self-terminates at the (111) planes as shown. (d) A small Si chip is cut from the wafer to serve as a pedestal for mounting the cantilever in the AFM [5.4]

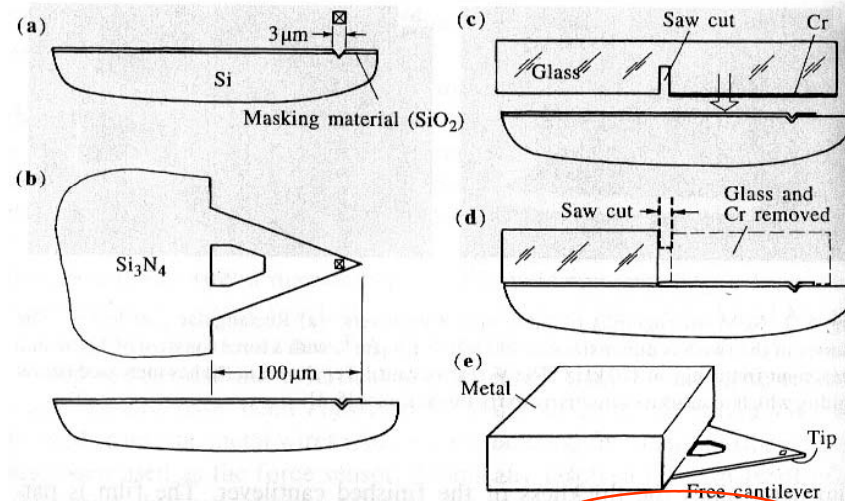
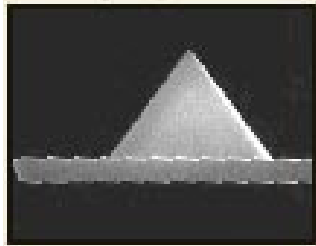


Fig. 5.4a-e. Fabrication of Si_3N_4 microcantilevers with integrated pyramidal tips (a) to (e) illustrate the steps in the fabrication process, see text [5.4]

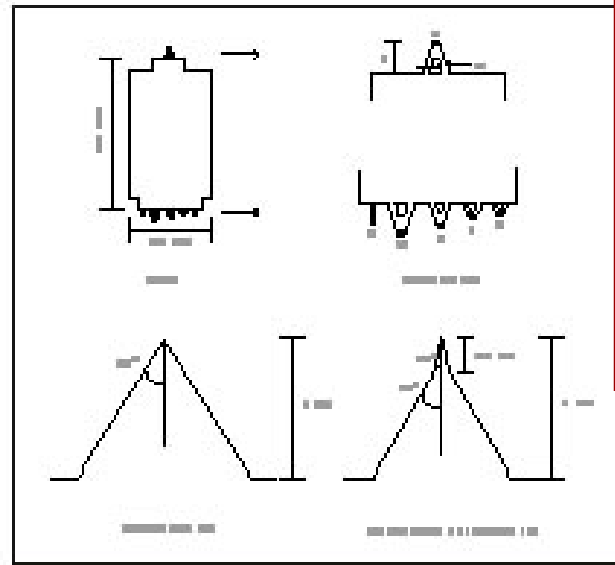
Examples of commercial cantilevers

FEATURES:

- Compatible with all major AFM brands.
- Typical radius of curvature: sharpened tips: < 20 nm, unsharpened tips: < 50 nm.
- Available with gold coating for high reflectivity.
- Recessed corners for easy sample approach.
- The widest range of spring constants commercially available on a single chip.



Thermomicroscopes Microlevers are ideal for all contact imaging modes, force modulation microscopy, and liquid operation. The range in force constants enable users to image soft samples in contact as well as high load force vs. distance spectroscopy.



Many different cantilevers are commercially available

They are different for:

- Dimensions and shape, typ 0.1-0.5 mm:
- Elastic constant (materials and design, typ 0.05-50 N/m;
- Tip coating (conductive, super-hard, etc.)

Typical Mechanical Characteristics

Cantilever type	A - triangular	B - rectangular	C - triangular	D - triangular	E - triangular	F - triangular
Standard mode of operation	Contact					
Cantilever length	180 µm	200 µm	320 µm	220 µm	140 µm	85 µm
Cantilever width	18 µm	20 µm	22 µm	22 µm	18 µm	18 µm
Cantilever thickness	0.6 µm	0.6 µm	0.6 µm	0.6 µm	0.6 µm	0.6 µm
Force Constant	0.05 N/m	0.02 N/m	0.01 N/m	0.03 N/m	0.10 N/m	0.50 N/m
Resonant Frequency	22 kHz	15 kHz	7 kHz	15 kHz	38 kHz	120 kHz

Ordering Information

Microlevers	Sharpened		Unsharpened	
	Gold coated*	Uncoated	Gold coated*	Uncoated
Half wafer - (250 chips)	MSCT-AUHW	MSCT-NCHW	MLCT-AUHW	MLCT-NCHW
Unmounted - (25 chips)	MSCT-AUNM	MSCT-NCNM	MLCT-AUNM	MLCT-NCNM
Mounted - (25 chips)	MSCT-AUMT-A	MSCT-NDMT-A	MLCT-AUMT-A	MLCT-NDMT-A
Mounted - (25 chips)	MSCT-AUMT-BF	MSCT		F

* Not for use with AutoProbe MS systems

Cantilever choice depends for instance on:

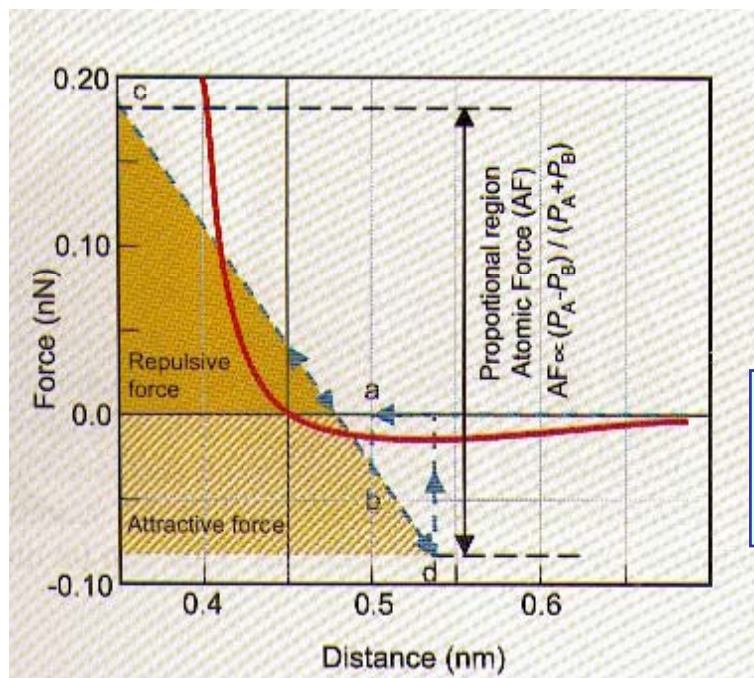
- Operation mode (contact/non contact);
- Quantities to be probed (e.g., if an electric field is needed, a conductive tip has to be used);
- Possible material manipulation (e.g., nanoindentation requires super-hard tips)

Basics of tip/sample interaction

When the tip is approached to the sample (at sub-nm distance!), forces depend roughly on van der Waals interaction between the apical tip atoms and the surface

At “large” distance forces are weakly attractive, at “short” distance they are repulsive

Surface topography (height variations) can be sensed by monitoring the force, i.e., the **cantilever deflection**



When tip/sample distance is kept in the repulsive region, **contact operating mode** is achieved

When tip/sample distance is kept (*mostly*) in the attractive region, **non-contact operating mode** is achieved

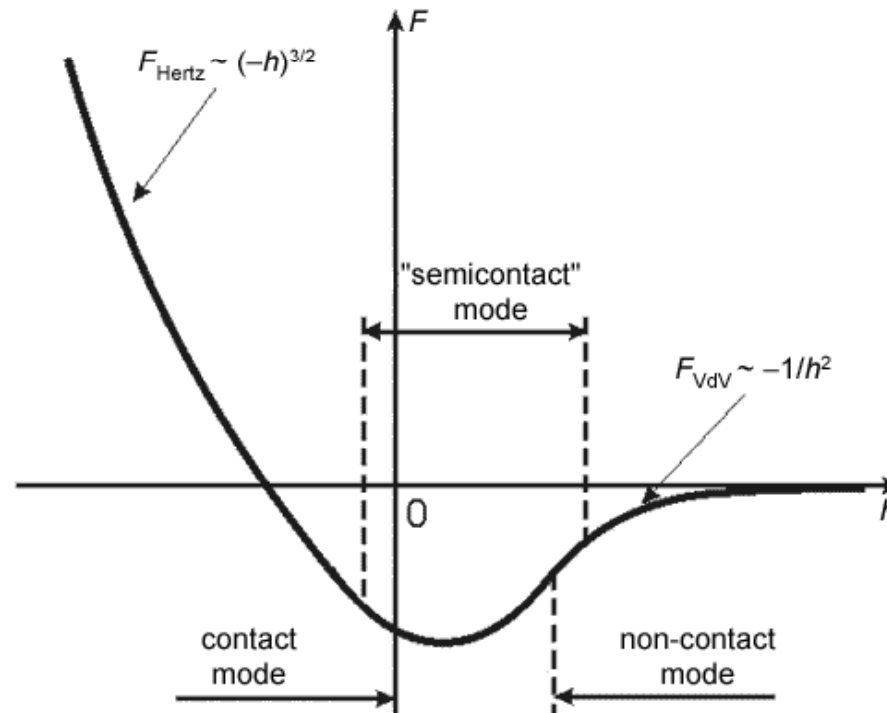
Tip/sample forces

Sample investigation is available thanks to the forces acting between a cantilever and a surface. They are quite different. One or another force dominate at different tip-sample separations.

- During contact and the surface deformation by the cantilever, the elastic repulsion force dominates; this approximation is called the **Hertz model** and is considered in the chapter "[Elastic interactions. The Hertz problem](#)".
- At tip-sample separations of the order of several tens of angstrom the major interaction is the intermolecular interaction called the **Van der Waals force** (see chapter "[The Van der Waals force](#)").
- At the same distance between the tip and the sample and in the presence of liquid films, the interaction is influenced much by **capillary and adhesion forces**. The range of capillary forces considered in the chapter "[Capillary forces](#)" is determined by the liquid film thickness.
- At larger separations the **electrostatic interaction** starts to dominate. It is described in chapter "[Electrostatic force microscopy](#)".
- At separations of the order of a thousand of angstroms **magnetic forces** considered in the chapter "[Magnetic force microscopy](#)" prevail.



Various kind of forces do cooperate in providing the typical force vs distance behavior experienced in AFM



A few words on elastic forces

When the cantilever and the sample are in contact, elastic forces start to act giving rise to both the sample and tip deformations which can affect the acquired image. To properly interpret the results and choose the measuring mode one should have a clear idea of elastic interactions in contact and "semicontact" modes.

Such consideration is necessary in order to:

- avoid tip or sample damage during scanning - even at low loading force the pressure in a contact zone can exceed the strength limit because contact area is very small.
- reconstruct properly the sample surface topography basing on the acquired image profile in case when surface features are of the same size as the tip curvature radius.
- analyze forces in the "semicontact" mode at a moment of the tip contact with the surface which directly affect the cantilever oscillation and are one of the damping reasons.

Elastic deformations in the contact zone (the Hertz problem).

Let us consider first only the elastic force. **The Hertz problem** is deformations determination at local contact of bodies under load F action.

We have to adopt some simplifying assumptions [1].

1. Suppose that both the cantilever and sample materials are isotropic, i.e. their elastic properties are described only by two pairs of parameters – Young's moduli E, E' and Poisson ratios μ, μ' . (For the anisotropic materials the number of such independent elastic characteristics can reach 21).
2. Assume that in the vicinity of the contact point the undeformed parts of bodies surface in perpendicular planes orthogonal to the plane in the given point (**Fig. 1**) are described by two curvature radii r_1, r_2 (for the tip) and r_1', r_2' (for the studied sample area).
3. Deformations are small compared to surfaces curvature radii.

The change in the probe vertical position during scanning in the contact mode produces profile which can differ much from the real surface topography. One of the reasons for that is the elastic deformation of the tip and the sample. For example, the decrease in the organic molecules vertical dimensions was experimentally established. Because these materials are very soft, the probe "indents" protrusions on their surfaces (See [Appendix 3](#) and [chapter 2.5.1](#)).

The second reason for the difference between scan profile and real surface geometry is the tip-sample convolution. Its consideration is important when studying small (of the order of the tip curvature radius) surface features. A finite tip dimension results in the lack of the ability to probe narrow cavities on the sample surface thus decreasing their depth and width. Similarly, convex features image appears wider. The convolution phenomenon is best understood from **Fig. 1**.

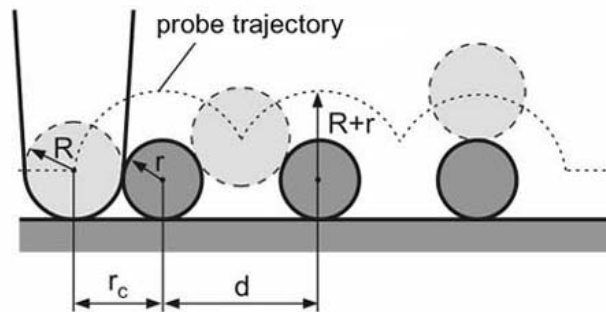


Fig. 1. Tip convolution during scanning. The scan profile can differ much from real surface geometry.

The Hertz problem solution relates the loading force F and the penetration depth h :

$$F = \frac{K\alpha^3}{R} = Kh^{\frac{3}{2}} \frac{1}{R^{\frac{1}{2}}} \quad (3)$$

Accordingly, the pressure is the following function of the force:

$$P = \frac{F}{\pi\alpha^2} = \frac{1}{\pi} \sqrt[3]{\frac{FK^2}{R^2}} \quad (4)$$

The given solution for the case of two spherical bodies contact includes one important special case of the flat sample contact with the tip having curvature radius R ($r = R, r' = \infty$).

Let us depict the Hertz problem solution, i.e. the dependence of the penetration depth (horizontal axis) upon the loading force (vertical axis) for positive h . In **Fig. 3**, the rising branch corresponds to the Hertz problem solution.

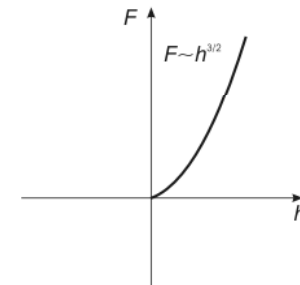


Fig. 3. Force F depending on penetration depth h (graph of the Hertz problem solution).

If one assumes the simultaneous effect of convolution and deformation, it becomes clear how much the image profile can differ from the real topography. In [Appendix 4](#) it is demonstrated that the acquired image needs to be analyzed and even computer processed in order to obtain the sample real topography.

Non-elastic conservative contact forces.

As tip makes contact with the sample, some other forces arise besides the elastic one. For example, the [Van der Waals interaction](#) (revealed not only when two bodies touch but within some distance between them) leads to the contact pressure decrease because Van der Waals forces in contrast to elastic ones are attractive but not repulsive.

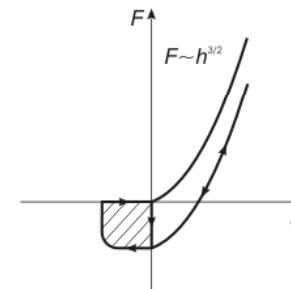


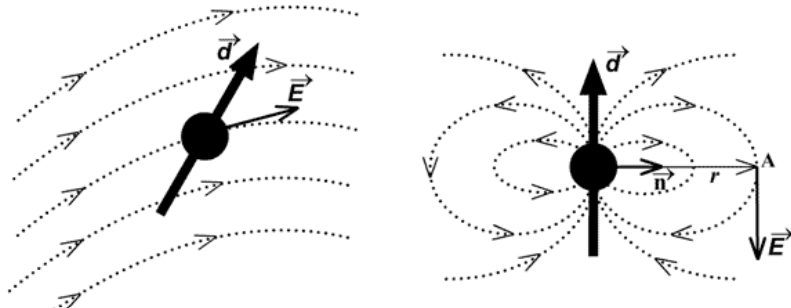
Fig. 2. Plots of force F vs. penetration depth h . Shown are the Hertz problem solution as well as solution with a hysteresis loop accounting for the nonconservative forces.

A few words on van der Waals I

The Van der Waals force or the intermolecular attractive force has three components of slightly different physical nature but having the same potential dependence on the intermolecular distance $\sim 1/r^6$. This lucky circumstance allows to compare directly constants of interaction that correspond to three Van der Waals force components because proportions between them will be held constant at different r magnitudes. Constants at $1/r^6$ multiplier will differ for various materials.

$$W = W_{\text{orient}} + W_{\text{ind}} + W_{\text{disp}} \sim 1/r^6 \quad (1)$$

All three Van der Waals force components are based on dipoles interaction, therefore we should remember two basic formulas:



the energy of dipole \mathbf{d} placed in field \mathbf{E} is [1]:

$$W_D = -\mathbf{d}\mathbf{E} \quad (2)$$

and the electric field produced by the dipole \mathbf{d} is [1]:

$$\mathbf{E} = \frac{3(\mathbf{nd})\mathbf{n} - \mathbf{d}}{r^3}, \quad |\mathbf{E}| \sim \frac{1}{r^3} \quad (3)$$

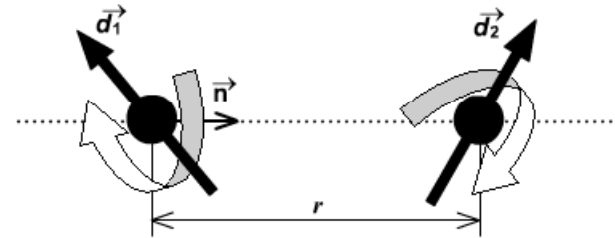
where \mathbf{n} – unit vector directed from the point at which the energy is determined to the dipole.

The orientational interaction (or the Casimir force) arises between two polar molecules each of which has the electric dipole moment. In accordance with (2), (3) the interaction energy of dipoles \mathbf{d}_1 and \mathbf{d}_2 separated by distance r

$$W_D = \frac{\mathbf{d}_1 \mathbf{d}_2 - 3(\mathbf{d}_1 \mathbf{n})(\mathbf{d}_2 \mathbf{n})}{r^3} \sim \frac{1}{r^3} \quad (4)$$

depends sufficiently upon the molecules relative position. Here \mathbf{n} is the unit vector directed along the line between molecules.

In order to reach the potential minimum, dipoles tend to align along the common axis (Fig. 1). The thermal motion, however, breaks this order. To determine the "resulting" orientation potential W_{orient} one should average statistically interactions over all possible orientations of molecules pair. Notice that in accordance with the Gibbs distribution $\exp(-W/kT)$, which gives the probability of the system being in the state with energy W at temperature T , the energetically advantageous orientations are preferable. That is why despite the isotropy of possible mutual orientations, the average result will be nonzero.



Averaging with the use of the Gibbs distribution is performed in accordance with the following formula:

$$W_{\text{orient}} = \frac{\int W_D \exp\left(-\frac{W_D}{kT}\right) dv}{\int \exp\left(-\frac{W_D}{kT}\right) dv} \quad (5)$$

where, for the sake of normalization, the denominator is the statistical sum and v is the integration parameter providing enumeration of all the system possible states (a pair of dipoles mutual orientations).

If $W_D \ll kT$ the exponent can be approximated by the series expansion:

$$\exp\left(-\frac{W_D}{kT}\right) \approx 1 - \frac{W_D}{kT} \quad (6)$$

so the energy of orientation interaction is approximated as:

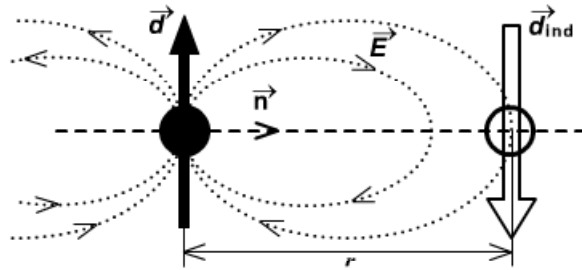
$$W_{\text{orient}} \sim \frac{\int W_D dv + \int \frac{W_D^2}{kT} dv}{\int dv + \int W_D dv} \quad (7)$$

On performing integration it can be shown that $\int W_D dv = 0$, thus, $W_{\text{orient}} \sim W_D^2$. Introducing constant A_1 in accordance with (4), we finally have:

$$W_{\text{orient}} = \frac{\text{const}}{kT} \frac{1}{r^6} = -\frac{A_1}{r^6} \quad (8)$$

A few words on van der Waals II

The **induction interaction** (or the **Debye force**) arises between polar and nonpolar molecules. Electric field \mathbf{E} generated by dipole \mathbf{d}_1 polarizes the other molecule (Fig. 2). The induced moment calculated in the first order of the quantum perturbation theory is equal to $\mathbf{d}_{ind} = \chi \mathbf{E}$ where χ stands for the molecule polarizability.



Then, the potential of induction interaction is computed as follows:

$$W_{ind} = \mathbf{d}_{ind} \mathbf{E} = \chi \mathbf{E}^2 = \chi \frac{-3(\mathbf{n} \mathbf{d}_1)^2 + \mathbf{d}_1^2}{r^6} = -\frac{\chi \mathbf{d}_1^2}{2r^6} \sim \frac{1}{r^6} \quad (9)$$

Thus, this kind of interaction also "universally" depends on $W = W_{orient} + W_{ind} + W_{disp} \sim 1/r^6$ though having the other reason and the other constant.

It should be noted that in liquids and solids the polarized molecule experiences the symmetric influence of many neighbor molecules, the induction interaction being strongly compensated by their action. The result is that the real induction interaction is estimated as:

$$W_{ind} \sim \frac{1}{r^n}, n = 8 + 13 \quad (10)$$

Obviously, the force is determined by

$$\mathbf{F} = -\text{grad} W_D, W_{disp} = -\frac{A_3}{r^6} \quad (13)$$

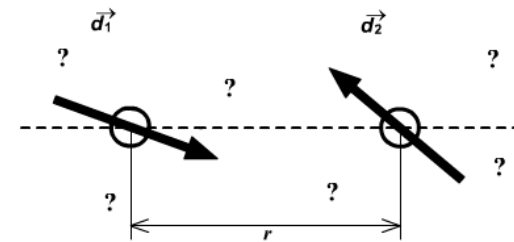
Estimations of the Van der Waals attraction for AFM studies in the contact mode give: $F_{vdV} \sim 10^{-8} + 10^{-9}$ N.

Van der Waals interaction is based on different dipole/dipole interaction mechanisms, all leading

to a r^{-6} behavior

This results into a r^{-m} force on the cantilever depending on specific tip shape and distance

The **dispersion interaction** (or the **London force**) is a prevailing one because it involves nonpolar molecules as well. This third term in (1) is always presented that is why it is the major one.



1. 3. Due to the quantum uncertainty, nonpolar molecules have "momentary" dipole moments, interaction between which is of the second order of smallness of the perturbation theory.

In a system of nonpolar molecules the electrons wave function Ψ is such that average values of dipole moments in any state n are equal to zero: $\langle \psi_n | \mathbf{d}_{1,2} | \psi_n \rangle = 0$. However, nondiagonal matrix elements $\langle \psi_n | \mathbf{d}_{1,2} | \psi_m \rangle$ are nonzero. Moreover, the second quantum mechanical correction to the interaction energy calculated as is known [2] according to the formula below, is nonzero too:

In a system of nonpolar molecules the electrons wave function Ψ is such that average values of dipole moments in any state n are equal to zero: $\langle \psi_n | \mathbf{d}_{1,2} | \psi_n \rangle = 0$. However, nondiagonal matrix elements $\langle \psi_n | \mathbf{d}_{1,2} | \psi_m \rangle$ are nonzero. Moreover, the second quantum mechanical correction to the interaction energy calculated as is known [2] according to the formula below, is nonzero too:

$$W_n^{(2)} = \sum_{n,m} \frac{|\langle \psi_n | W | \psi_m \rangle|^2}{\epsilon_n - \epsilon_m} \quad (11)$$

where perturbation W is given by (4), ϵ_n, ϵ_m – energies of the system of two molecules in arbitrary states n and m .

In a certain sense, "momentary" magnitudes of dipole moments (at zero average value) are nonzero and they interact (Fig. 3). In the second order of smallness the averaged magnitude of such "momentary" potential is not already vanished and namely this is the potential of dispersion interaction.

Correction (11) as is seen, is proportional to the square of perturbation W_D . From this it is clear that

$$W_{disp} \sim W_D^2, W_{disp} = -\frac{A_3}{r^6} \quad (12)$$

Constant $A_3 = \frac{3I_1 I_2}{2(I_1 + I_2)} \chi_1 \chi_2$ is called the Hamaker constant (here I_1, I_2 – ionization potentials, χ_1, χ_2 – molecules polarizability).

The classical interpretation of this interaction is as follows. The dipole moment of one molecule arisen from fluctuations, generates field which, in turn, polarizes the second molecule. The already nonzero field of the second molecule polarizes the first one. The potential of this peculiar system with a "positive feedback" is calculated similarly to the induction interaction.

Not to forget: adhesion/capillary effects

Let us examine the effect of the surface tension on AFM measurements. [1] At the moment of a cantilever contact with a liquid film on a flat surface, the film surface reshapes producing the "neck". The water wets the cantilever surface (Fig. 1) because the water-cantilever contact (if it is hydrophilic) is energetically advantageous as compared to the water-air contact. Notice that in such cases the contact angle is always less than 90° .

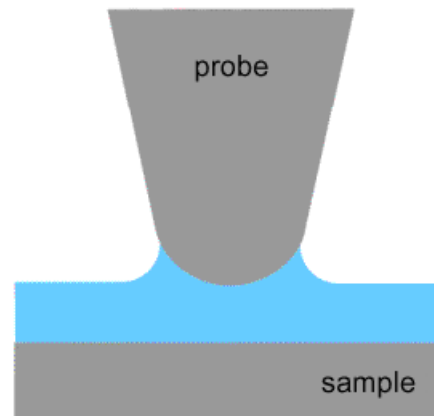


Fig. 1. "Neck" formation.

It is intuitively clear that the neck curved surface will tend to flatten that is available only at the expense of the cantilever pulling down. This means that the cantilever attracts to the sample.

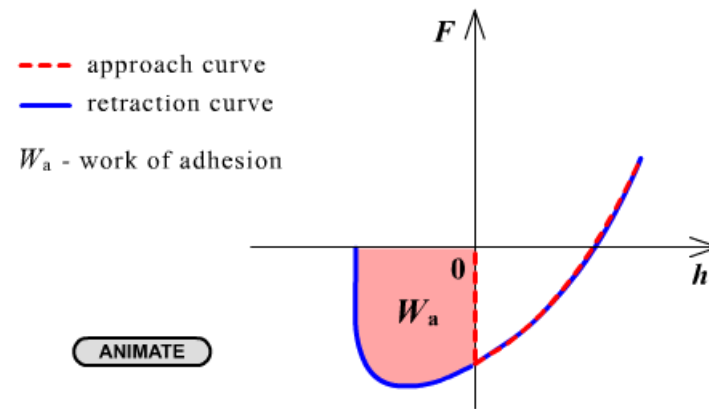
Calculation of this attraction force is a simple task. Let the tip curvature radius be much larger than other characteristic dimensions of the case. In Fig. 2 the following designations are introduced: D – tip-sample separation, d – "immersion depth", h – film thickness, ρ_1 – lesser curvature radius of the liquid surface, ρ_2 – tip-liquid contact area radius.

We will not concentrate attention on d value determination. For the estimation purpose we will use the maximum value of the capillary attraction force that takes place at $D = 0$. In this case the unknown parameter d vanishes:

$$F_{\text{cap}} = F_{\text{max}} = 4\pi R \sigma \cos \theta \quad (5)$$

Taking into account that cantilever radius R is 10 nm , water surface tension at 20°C is equal to 0.073 N/m and the contact angle is small i.e. $\cos \theta$ is close to 1, we get the following estimation: $F_{\text{cap}} \sim 10^{-8} - 10^{-9} \text{ N}$. Thus, the capillary force by the order of magnitude is the same as the Van der Waals interaction and the electrostatic force.

During the cantilever approach-retraction cycle, the hysteresis arises. At the upward move the neck stays longer because the cantilever surface is already wetted and the liquid neck goes with the tip. As bonds break, the capillary force stops to act and the cantilever suddenly returns into its undeflected state.



Adhesion effects can further affect the interaction (unless UHV operation is performed!)

Scanning Force Microscopy

3.2 The Operation Principle of Scanning Force Microscope

The main electronic components of the SFM are the same as for the STM, only the topography of the scanned surface is reconstructed by analysing the deflection of the tip at the end of a spring. Today, the interferometrical and optical lever method dominate commercial SFM apparatus. The most common method for detecting the deflection of cantilever is by measuring the position of a reflected laser-beam on a photosensitive detector. The principle of this optical lever method is presented in Figure 18 a. Without

cantilever displacement both quadrants of the photodiode (A and B) have the same irradiation $P_A = P_B = P/2$ (P represents the total light intensity). The change of the irradiated area in the quadrants A and B is a linear function of the displacement

$$\delta \propto \Delta d = 2 \sin(\Theta) \cdot S_2 = 2\Theta \cdot S_2 = 3S_2 \cdot \delta/L \quad (10)$$

For small angles $\sin(\Theta) \approx \Theta$ and Θ may be evaluated from the relation $\Theta = 3\delta/2L$ (Figure 18b). For P_A and P_B one would get approximately $P_A = P/2 \cdot (d + \Delta d)/2$ and $P_B = P/2 \cdot (d - \Delta d)/2$. Using the simple difference between P_A and P_B would lead to

$\Delta P = P \cdot 3S_2\delta/(Ld)$ but in this case one cannot distinguish between the displacement δ of the cantilever and the variation in the laser power P . Hence the normalised difference is used, which is only dependent of δ :

$$\frac{P_A - P_B}{P_A + P_B} = \delta \cdot \frac{3S_2}{Ld} \quad (11)$$

The "lever amplification" $\Delta d/\delta = 3S_2/L$ is about a factor of one thousand. On the basis of this kind of technique one is able to detect changes in the position of a cantilever of the order of 0.01 nm.

For large distances between the tip and the sample the bending of the cantilever by attractive forces is negligible. After the cantilever is brought closer to the surface of the sample (point "a" Figure 18c) the van der Waals forces induce a strong deflection of the cantilever and, simultaneously, the cantilever is moving towards the surface. This increases the forces on the cantilever, which is a kind of positive feedback and brings the cantilever to a direct contact with the sample surface (point "b"). However, when the cantilever is brought even closer in contact to the sample, it actually begins to bend in the opposite direction as a result of a repulsive interaction ("b-c"). In the range ("b-c") the position of the laser beam on both quadrants, which is proportional to the force, is a linear function of distance. On reversal this characteristic shows a hysteresis. This means that the cantilever loses contact with the surface at a distance (point "d") which is much larger than the distance on approaching the surface (point "a").

Up to now, the actual probe, i.e. the tip of the leaf spring, has not been discussed in detail. Its preparation is particularly demanding since the tip and the sensitive spring should be one piece. Moreover, the cantilever should be as small as possible. Nowadays, such scanning tips are commercially available (in contrast to the tunnelling tips, which you should prepare yourself). Figure 19 shows such a spring with tip (cantilever) made of Si. The characteristic parameters of a cantilever has been presented in Figure 18b. The spring constant $k = Ead_c^3/4L^3 \sim 0.1 - 10 \text{ N/m}$ of the cantilever enables topographical analysis with atomic resolution.

For the realisation of a scanning force microscope, the force measurement must be supplemented by a feedback control, in analogy to the scanning tunnelling microscope. The controller keeps the amplitude of the vibration of the cantilever (the tip), and thus also the distance, constant. During scanning the feedback controller retracts the sample with the scanner of a piezoelectric ceramic or shifts towards the cantilever until the vibration amplitude has reached the setpoint value again. The principle of height regulation is exactly the same as for the scanning tunnelling microscope. The scanning force micrographs thus show areas of constant effective force constant. If the surface is chemically homogeneous and if only van der Waals forces act on the tip, the SFM image shows the topography of the surface.

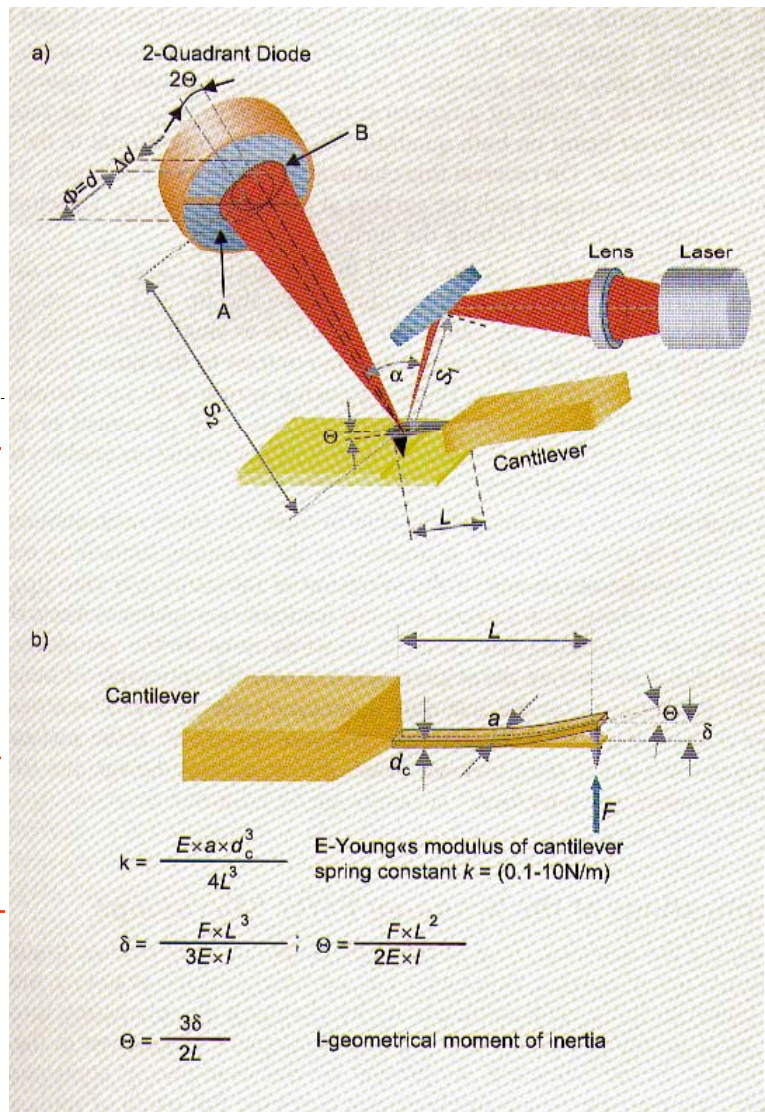


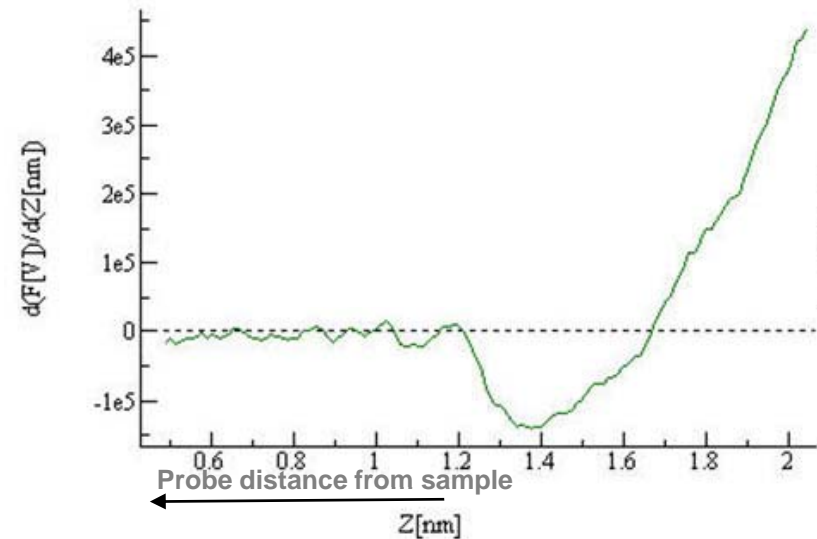
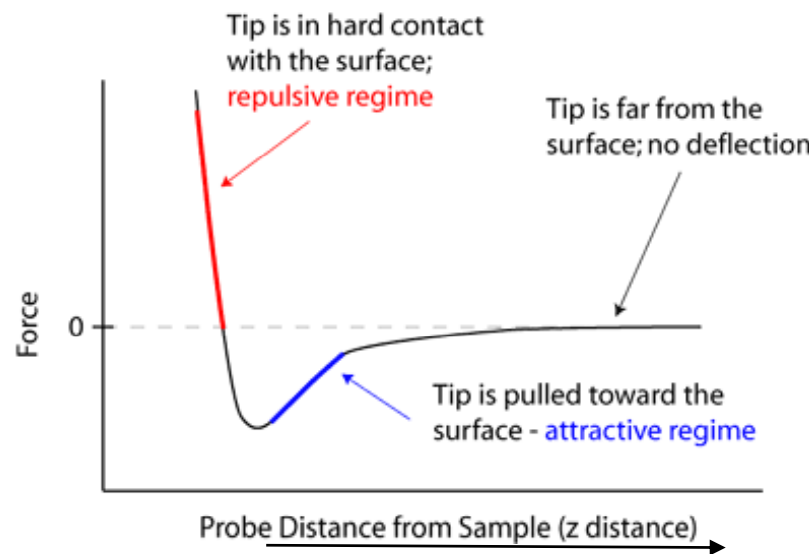
Figure 18: The amplification of the cantilever motion through the optical lever arm method. (a) Optical laser path in the standard AFM set-up. (b) Cantilever beam in bending. (c) Cantilever force as a function of the distance tip – sample distance.

An optical lever method is used to detect the cantilever deflection

Force vs distance curves

In the approaching step, force (i.e., cantilever deflection) vs distance plots have a typical behavior

Force vs distance curves can be used to get local information on the mechanical properties of the surface (*force spectroscopy*)



Note: we are discussing of the **contact mode operation** and tip might penetrate into the sample (*as in nanoindentation – we will see later!*)

Contact mode of operation

3.1 Theoretical Principles of the Scanning Force Microscope

As already mentioned above, van der Waals forces lead to an attractive interaction between the tip on the spring and the sample surface. Figure 15 shows schematically the van der Waals potential between two atoms. The potential can be described in a simpler classical picture as the interaction potential between the time dependent dipole moments of the two atoms. Although the centres of gravity of the electronic charge density and the charge of nucleus are exactly overlapping on a time average, the separation of the centres of gravity is spatially fluctuating in every moment. This produces statistical fluctuations of the atoms' dipole moments. The dipole moment of an atom can again induce a dipole moment in the neighbouring atom and the induced dipole moment acts back on the first atom. This creates a dipole-dipole interaction on basis of the fluctuating dipole moments. This interaction decreases with d^6 in the case of small distances d (Lenard-Jones potential). At larger distances, the interaction potential decreases more rapidly (d^7). This arises from the fact that the interaction between dipole moments occurs through the exchange of virtual photons. If the transit time of the virtual photon between atoms 1 and 2 is longer than the typical fluctuation time of the instantaneous dipole moment, the virtual photon weakens the interaction. This range of the van der Waals interaction is therefore called retarded, whereas that at short distances is unretarded.

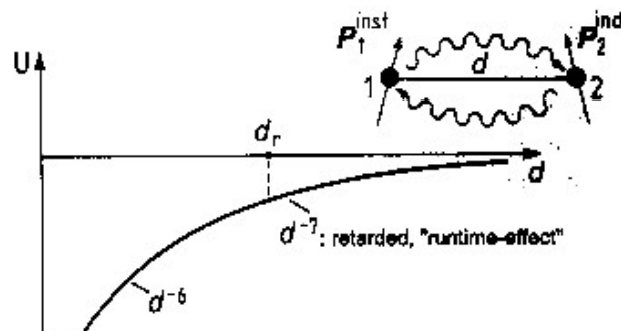


Figure 15: The van der Waals potential U between two atoms. d_r is the critical distance above which the transit time effects weaken the interaction [23].

Contact mode is suitable for rather rigid surfaces

The scanning force microscope is not based on the interaction of individual atom only. Both the sample and the tip are large in comparison to the distance. In order to obtain their interaction, all forces between the atoms of both bodies need to be integrated. The result of this is known for simple bodies and geometries. In all cases, the summation leads to a weaker decrease of the interaction. A single atom at distance d relative to a half-space leads to an interaction potential of

$$U = -\frac{C\pi\rho}{6} \cdot \frac{1}{d^3} \quad (7)$$

where C is the interaction constant of the van der Waals potential and ρ the density of the solid. C is basically determined by the electronic polarizabilities of the atoms in the half-space and of the single atom. If one has two spheres with radii R_1 and R_2 at distance d (distance between sphere surfaces) one obtains an interaction potential of

$$U = -\frac{AR_1R_2}{6(R_1+R_2)} \cdot \frac{1}{d} \quad (8)$$

where A is the so-called Hamaker constant. It is materials specific and essentially contains the densities of the two bodies and the interaction constant C of the van der Waals potential. If a sphere with radius R has a distance d from a half-space, an interaction potential of

$$U = -\frac{AR}{6} \cdot \frac{1}{d} \quad \text{Realistic tip/surface potential} \quad (9)$$

is obtained from Eq. (8). This case describes the geometry in a scanning force microscope best and is most widely used. The distance dependence of the van der Waals potential thus obtained is used analogously to the distance dependence of the tunnel current in a scanning tunnelling microscope to achieve a high resolution of the scanning force microscope. However, since the distance dependence is much weaker, the sensitivity of the scanning force microscope is lower.

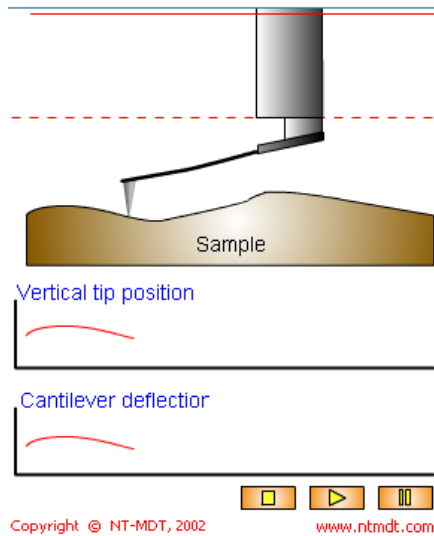
In the contact mode of operation, mechanical interaction leads to tip displacement, i.e., to cantilever deflection related to topography changes

As in STM (constant gap), typical operation foresees a feedback system, acting on the Z direction of the piezoscanner, which keeps constant the cantilever deflection during the scan

The "error signal" of the feedback system provides a topography map (with a calibrated sub-nm space resolution)

Operation modes (AFM contact)

The most straightforward AFM operation mode involves “**contact**” (repulsive) forces
 Constant height and **constant force** configurations are possible (the latter, the most common, is based on feedback)
 Major drawback: surface degradation, especially with soft matter



In **Contact mode** of operation the cantilever deflection under scanning reflects repulsive force acting upon the tip.

Repulsion force F acting upon the tip is related to the cantilever deflection value x under Hooke's law: $F = -kx$, where k is cantilever spring constant. The spring constant value for different cantilevers usually vary from 0.01 to several N/m.

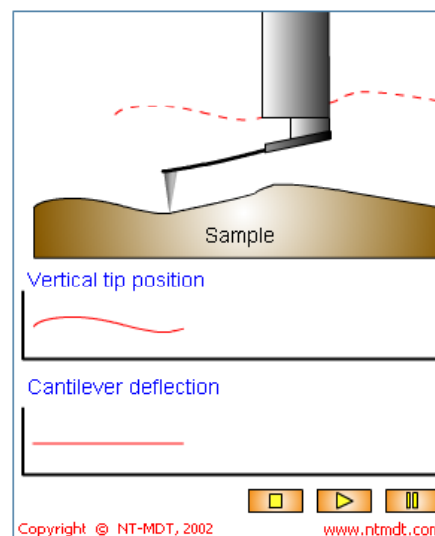
In our units the vertical cantilever deflection value is measured by means of the optical registration system and converted into electrical signal DFL. In contact mode the DFL signal is used as a parameter characterizing the interaction force between the tip and the surface. There is a linear relationship between the DFL value and the force. In Constant Height mode of operation the scanner of the microscope maintains fixed end of cantilever on the constant height value. So deflection of the cantilever under scanning reflects topography of sample under investigation.

Constant Height mode has some advantages and disadvantages.

Main advantage of Constant Height mode is high scanning speeds. It is restricted only by resonant frequency of the

cantilever.

Constant Height mode has also some disadvantages. Samples must be sufficiently smooth. When exploring soft samples (like polymers, biological samples, Langmuir-Blodgett films etc.) they can be destroyed by the scratching because the probe scanning tip is in direct contact with the surface. Thereunto under scanning soft samples with relatively high relief the pressure upon the surface varies, simultaneously varies local flexure of sample surface. As a result acquired topography of the sample can prove distorted. Possible existence of substantial capillary forces imposed by a liquid adsorption layer can decrease the resolution.



In **Contact mode** of operation the cantilever deflection under scanning reflects repulsive force acting upon the tip.

Repulsion force F acting upon the tip is related to the cantilever deflection value x under Hooke's law: $F = -kx$, where k is cantilever spring constant. The spring constant value for different cantilevers usually vary from 0.01 to several N/m.

In our units the vertical cantilever deflection value is measured by means of the optical registration system and converted into electrical signal DFL. In contact mode the DFL signal is used as a parameter characterizing the interaction force between the tip and the surface. There is a linear relationship between the DFL value and the force. In Constant Force mode of operation the deflection of the cantilever is maintained by the feedback circuitry on the preset value. So vertical displacement of the scanner under scanning reflects topography of sample under investigation.

Constant Force mode has some advantages and disadvantages.

Main advantage of Constant Force mode is possibility to measure with high resolution simultaneously with topography some other characteristics - [Friction Forces](#), [Spreading Resistance](#) etc.

Constant Force mode has also some disadvantages. Speed of scanning is restricted by the response time of feedback system. When exploring soft samples (like polymers, biological samples, Langmuir-Blodgett films etc.) they can be destroyed by the scratching because the probe scanning tip is in direct contact with the surface. Thereunto under scanning soft unhomogeneous samples the local flexure of sample surface varies. As a result acquired topography of the sample can prove distorted. Possible existence of substantial capillary forces imposed by a liquid adsorption layer can decrease the resolution.

Locally probing the (repulsive) force allows for topography and morphology reconstruction

Non-contact modes of operation

The dynamic operation method of a scanning force microscope has proved to be particularly useful. In this method the nominal force constant of the van der Waals potential, i.e. the second derivative of the potential, is exploited. This can be measured by using a vibrating tip (Figure 16). If a tip vibrates at distance d , which is outside the interaction range of the van der Waals potential, then the vibration frequency and the amplitude are only determined by the spring constant k of the spring. This corresponds to a harmonic potential. When the tip comes into the interaction range of the van der Waals potential, the harmonic potential and the interaction potential are superimposed thus changing the vibration frequency and the amplitude of the spring.

This is described by modifying the spring constant k of the spring by an additional contribution f of the van der Waals potential. As a consequence, the vibration frequency is shifted to lower frequencies as shown in Figure 17. ω_0 is the resonance frequency without interaction and $\Delta\omega$ the frequency shift to lower values. If an excitation frequency of the tip of $\omega_m > \omega_0$ is selected and kept constant, the amplitude of the vibration decreases as the tip approaches the sample, since the interaction becomes increasingly stronger. Thus, the vibration amplitude also becomes a measure for the distance of the tip from the sample surface. If a spring with low damping Q^{-1} is selected, the resonance curve is steep and the ratio of the amplitude change for a given frequency shift becomes large.

In practice, small amplitudes (approx. 1 nm) in comparison to distance d are used to ensure the linearity of the amplitude signal. With a given measurement accuracy of 1 %, however, this means that the assembly must measure deflection changes of 0.01 nm, which is achieved most simply by a laser interferometer or optical lever method.

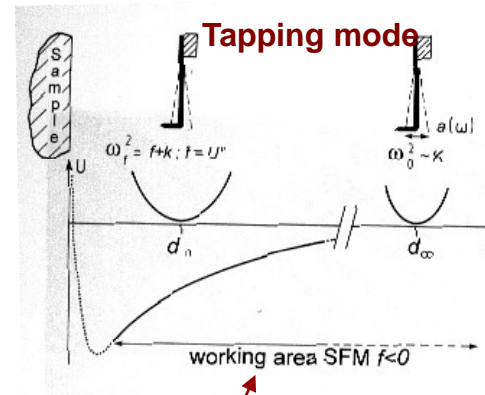


Figure 16: Schematic representation of the effect of the van der Waals interaction potential on the vibration frequency of the spring with tip. As the tip approaches the surface, the resonance frequency of the leaf spring is shifted. (from [23]).

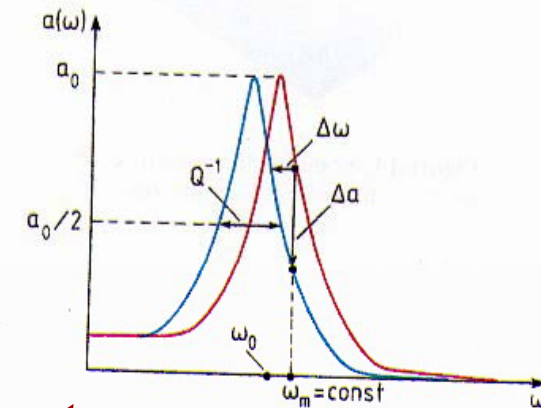


Figure 17: Resonance curves of the tip without and with interaction with a van der Waals potential. The interaction leads to a shift $\Delta\omega$ of the resonance frequency with the consequence that the tip excited with the frequency ω_m has a vibration amplitude $a(\omega)$ attenuated by Δa [23].

In **non-contact (tapping) mode**, the tip/sample distance is continuously modulated thanks to a vibrating tip

Tip vibration is typically achieved by using a piezoelectric transducer fed by an oscillating voltage and mechanically coupled to the cantilever

Oscillation frequency is typically set around the mechanical resonance frequency of the system (cantilever+tip), i.e., hundreds of kHz

The vibration reflects in an oscillation of the position-sensitive detector (multiquadrant diode) and amplitude is monitored

Tip/sample interaction leads to a **damping** (and **phase shift**) of the recorded oscillation when the distance gets small

Suitably conditioned electronic signals are sent into the feedback system in order to stabilize the distance and to derive the topography map

Non-contact modes suitable for “soft” surfaces

No sample preparation is needed!!

Effects on the cantilever resonance

Consider a cantilever oscillations when in addition to driving force ((1) in [chapter 2.2.3.3](#)), an external force $F_{ts}(z)$ acts on it. The equation of motion in this case is written as

$$\ddot{z} + 2\delta\dot{z} + \omega_0^2 z = A_0 \cos \Omega t + F_{ts}(z)/m \quad (1)$$

In a general case the steady-state solution of equation (1) is the sum of harmonics with frequencies divisible by a driving force frequency Ω :

$$z(t) = \sum_n A_n \cos(n\Omega t + \varphi_n) \quad (2)$$

In [chapter 2.2.3.4](#) we considered the particular case of equation (1) solution - **small oscillations** when the following condition is met

$$A_0 \ll \frac{m\omega_0^2}{\left\langle \frac{d^2 F_{ts}}{dz^2} \right\rangle} \quad (3)$$

where ω_0 – cantilever natural resonant frequency, $\left\langle \frac{d^2 F_{ts}}{dz^2} \right\rangle$ – mean of the second derivative of the tip-sample interaction force (averaged with respect to oscillations amplitude).

In practice, condition (3) is seldom met. However, utilizing numerical methods, one can show that even under weak condition (4), the character of steady-state oscillations will only slightly differ from harmonic (a major contribution is made only by the first harmonic)

condition
$$A_0 \leq \frac{m\omega_0^2}{\left\langle \frac{d^2 F_{ts}}{dz^2} \right\rangle} \quad (4)$$

solution
$$z(t) \sim A \cos(\Omega t + \varphi) \quad (5)$$

In contrast to the case of small oscillations where the steady-state condition is entirely determined by system parameters, the motion in the considered case depends on the initial state. That is, depending on the initial position of the cantilever relative to the equilibrium position, the character of the steady-state oscillations will vary (Fig. 1).

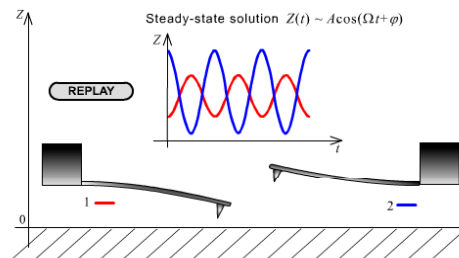


Fig. 1. Feasibility of several quasisteady-state solutions obtaining.

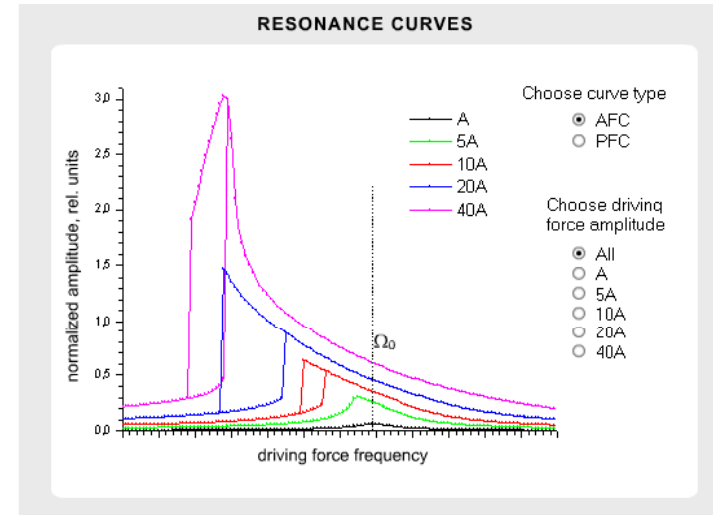
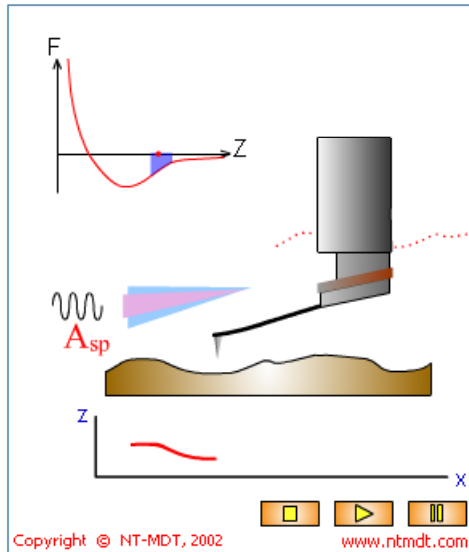


Fig. 2. Resonance curves in case of nonlinear oscillations.

Cantilever oscillations are strongly dependent on “damping” (both in terms of amplitude and frequency/phase)

Non-Contact mode.



The Non-Contact AFM (NC AFM), invented in 1987 [1], offers unique advantages over other contemporary scanning probe techniques such as contact AFM and STM. The absence of repulsive forces (presenting in **Contact AFM**) in NC AFM permits its use in the imaging "soft" samples and, unlike the STM, the NC AFM does not require conducting samples.

The NC AFM works via the principle "amplitude modulation" detection. The corresponding detection scheme exploits the change in the amplitude, A , of the oscillation of a cantilever due to the interaction of a tip with a sample. To the first order, the working of the NC AFM can be understood in terms of a force-gradient model [1]. According to this model, in the limit of small A , a cantilever approaching a sample undergoes a shift, df , in its natural frequency, f_0 , towards a new value given by

$$f_{\text{eff}} = f_0 (1 - F'(z)/k_0)^{1/2}$$

where f_{eff} is the new, effective resonance frequency of the cantilever of nominal stiffness k_0 in the presence of a force gradient $F'(z)$ due to the sample. The quantity z represents an effective tip-sample separation while $df = f_{\text{eff}} - f_0$ is typically negative, for the case of attractive forces.

If cantilever is initially forced to vibrate at a $f_{\text{set}} > f_0$, then the shift in the resonance spectrum of the cantilever towards lower frequencies will cause a decrease in the oscillation amplitude at f_{set} as the tip approaches the sample [1].

This change in A is used as the input to the NC-AFM feedback. To obtain a NC AFM image the user initially chooses a value A_{set} as the set-point such that $A_{\text{set}} < A(f_{\text{set}})$ when the cantilever is far away from the sample. The NC AFM feedback then moves the cantilever closer to the sample until its instantaneous oscillation amplitude, A , drops to A_{set} at the user-defined driving frequency f_{set} . At this point the sample can be scanned in the x - y plane with the feedback keeping $A = A_{\text{set}} = \text{constant}$ in order to obtain a NC AFM image. The NC AFM feedback brings the cantilever closer (on average) to the sample if A_{set} is decreased at any point, and moves the cantilever farther away from the sample (on average) if A_{set} is increased. Overall, the implication of the above model is that the NC AFM image may be considered, in the limit of small A , to be a map of constant interaction-force gradient experienced by the tip due to the sample.

The non-contact mode has the advantage that the tip never makes contact with the sample and therefore cannot disturb or destroy the sample. This is particularly important in biological applications.

References

1. J. Appl. Phys. 61, 4723 (1987).

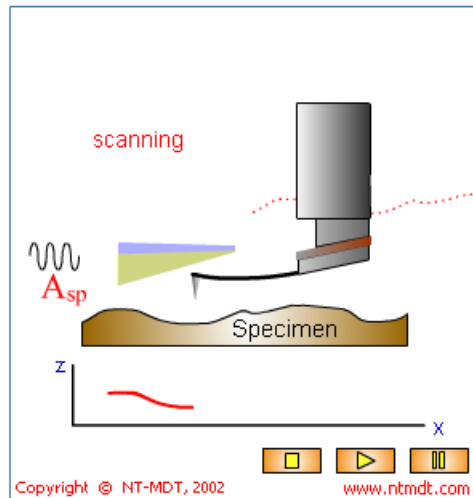
True non-contact mode

- ✓ Vertical oscillation (tapping) is applied to the tip, at a frequency close to its resonance
- ✓ Resonance frequency variations (and dephasing) are measured
- ✓ Feedback keeps the resonance frequency constant by changing the probe/sample distance, hence topography is reconstructed

Non-contact modes allow for analysis of soft surfaces

Examples of other operation modes

Semicontact mode.



Usage of [Scanning Force Microscopy](#) with oscillating cantilever was firstly anticipated by Binnig [1]. Earlier experimental realizations of scanning with oscillated cantilever was realized in works [2, 3]. It was demonstrated influence of the force gradients on the cantilever frequency shift and possibility of non-contact scanning sample surface. It must be noted also that Durig studied frequency shift of oscillating cantilever under influence of STM tip [4]. In [2] was demonstrated also possibility of materials sensing under abrupt decreasing of cantilever oscillation amplitude. Possibility of scanning sample surface not only in attractive but also in repulsive forces was demonstrated in [4]. Relatively small shift of oscillating frequency with sensing repulsive forces means that contact of cantilever tip with sample surface under oscillation is not constant. Only during small part of oscillating period the tip "feels" contact repulsive force. Especially it concerns to oscillations with relatively high

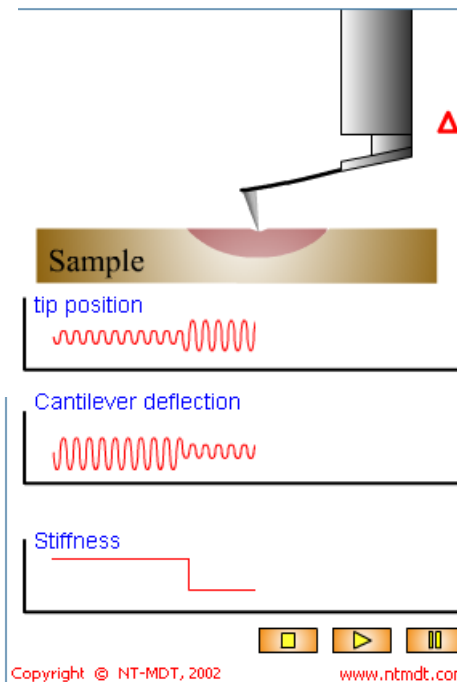
amplitudes. Scanning sample surface with cantilever oscillated in this manner is not non-contact, but intermittent contact. Corresponding mode of Scanning Force Microscope operation (Intermittent Contact mode) is in common practice.

The Intermittent Contact mode can be characterized by some advantages in comparison with [dc Contact mode](#). First of all, in this mode the force of pressure of the cantilever onto the surface is less, that allows to work with softer and easy to damage materials such as polymers and bioorganics. The semicontact mode is also more sensitive to the interaction with the surface that gives a possibility to investigate some characteristics of the surface - distribution of magnetic and electric domains, elasticity and viscosity of the surface.

Force modulation: an additional contrast mechanism related to material (mechanical) properties is found and exploited

Semicontact: the tip gets in "temporarily" contact thus combining advantages of contact and non-contact

Force Modulation mode.



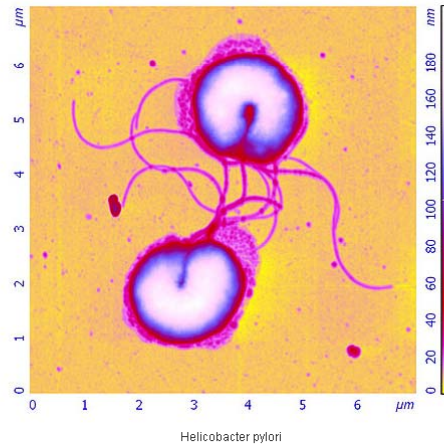
Under realization of Force Modulation mode (FM-mode) along with scanning of sample surface as in [Constant Force mode](#) (CFC-mode) the scanner (or the sample) executes a vertical periodic motion [1]. Under this periodic motion cantilever "feels out" the sample surface. At that the pressure of the probe tip on the sample surface does not remain constant but has periodic component, usually sinusoidal. In accordance with the local elasticity of the sample value of corresponding indentation will change under scanning. On the stiff areas of the sample surface depth of indentation will be smaller, and on the compliant areas - larger. Tracing of the sample surface relief height is conducted by the usage of the averaged cantilever deflection in the feedback circuit [2]. If values of the scanner vertical displacement Dz , the probe tip vertical displacement D and cantilever force constant κ_c are known, one can determine the local elasticity of the sample under investigation κ_s

$$\kappa_s = \kappa_c \cdot (Dz/D - 1)$$

In turn with known value of the local elasticity one can to determine the modulus of elasticity of the sample. It can be done with usage of the calibrating measurements or with usage of the Hertzian model [3]. Force Modulation mode is widely used in polymers, semiconductors, biological, especially in

composite materials investigations.

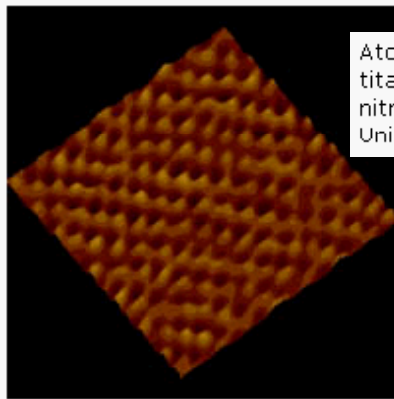
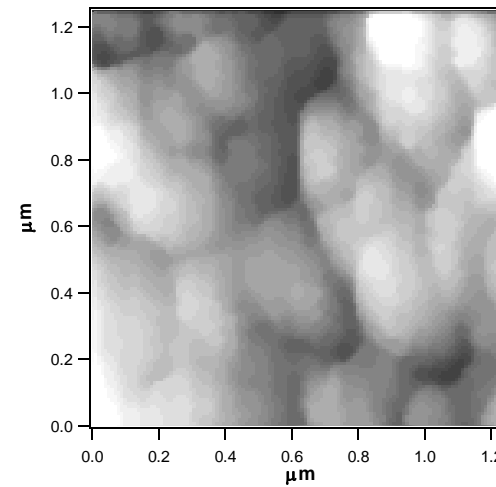
A very few examples of AFM images I



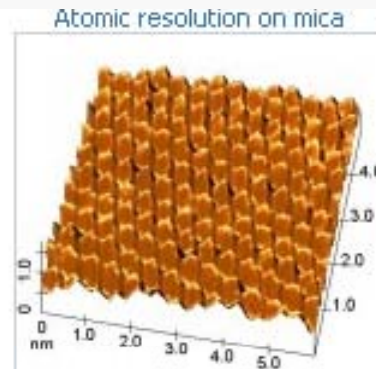
Mode: [Semicontact mode](#)
 SPM Model: [Solver P47H-PRO](#)
 Scan size: 7.2x7.2 μm
 Source MDT-file: [download \(1.01 Mb\)](#)

Conversion of two cells of bacterium *Helicobacter pylori* into coccoid forms. Polished silicone covered by polymer.

Image courtesy of Budashov I.A., Moscow State University, Institute of Biochemical Physics.
 Sample courtesy of Momynaliev K.T., Scientific Research Institute of Physical-Chemical Medicine, Moscow.

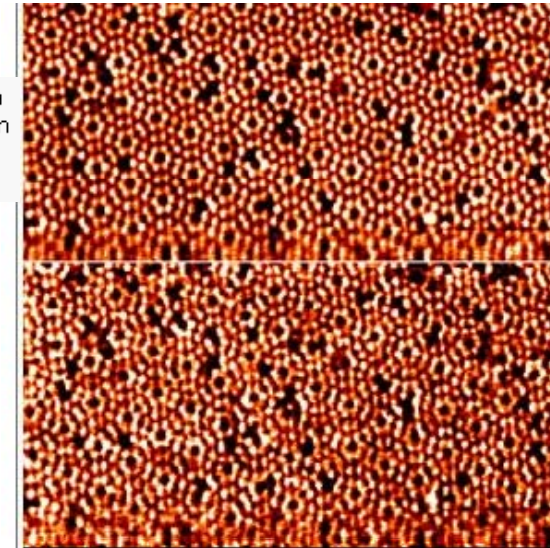


Atomic resolution image of the titanium oxide layer on top of a titanium substrate. Contact mode AFM in air, commercial silicon nitride cantilever. 5 nm scan courtesy P. Cacciafesta, University of Bristol, UK.



Muscovite is fairly common and is found in igneous, metamorphic and detrital sedimentary rocks. It has a layer-like structure of aluminum silicate sheets not strongly bonded, and they are held together by the K^+ ions. For further reading on this topic see the following publication: Gelatin on Mica Surfaces, *J Phys. Chem.* **94**, 4611-4617.

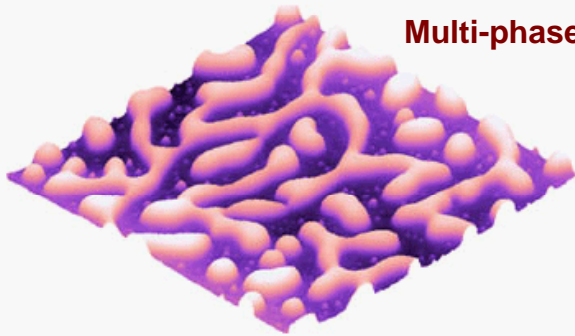
See <http://www.veeco.com>



Multi-mode AFM operation : with simultaneous measurement of the topography in STM mode (upper image) with atomic resolution on Si(111)7x7 using a conductive cantilever, and of the atomic scale variation of the force, i.e. cantilever deflection (lower image).

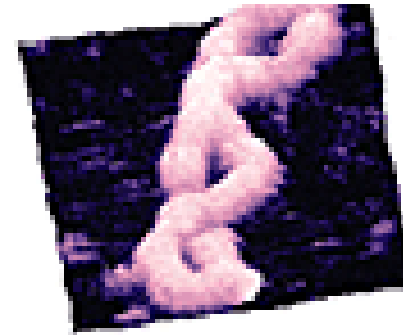
A very few examples of AFM images II

Multi-phase systems



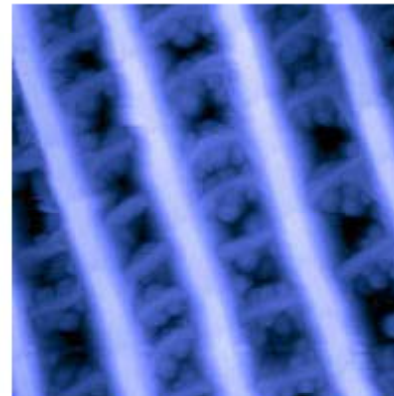
TappingMode AFM image of poly(styrene) and poly(methyl methacrylate) blend polymer film. The film was spin-cast on mica substrate from chloroform solution. The surface structure is resulted from the spinodal decomposition. The islands consist of a PMMS-rich phase while the surface matrix composes of a PS-rich phase. 3 μ m scan courtesy C. Ton-That, Robert Gordon University, U.K.

DNA Molecules

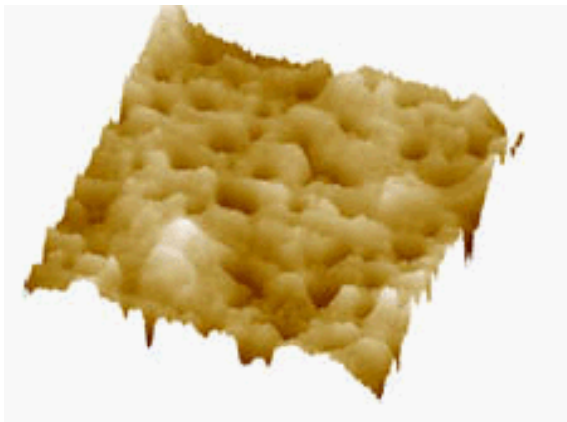


A high resolution of the SPM is able to discern very subtle features such as these two linear dsDNA molecules overlapping each other. 155nm scan. Image courtesy of W. Blaine Stine at email address stineb@stineb.pprd.abbott.com.

A Butterfly Wing Imaged in TappingMode AFM



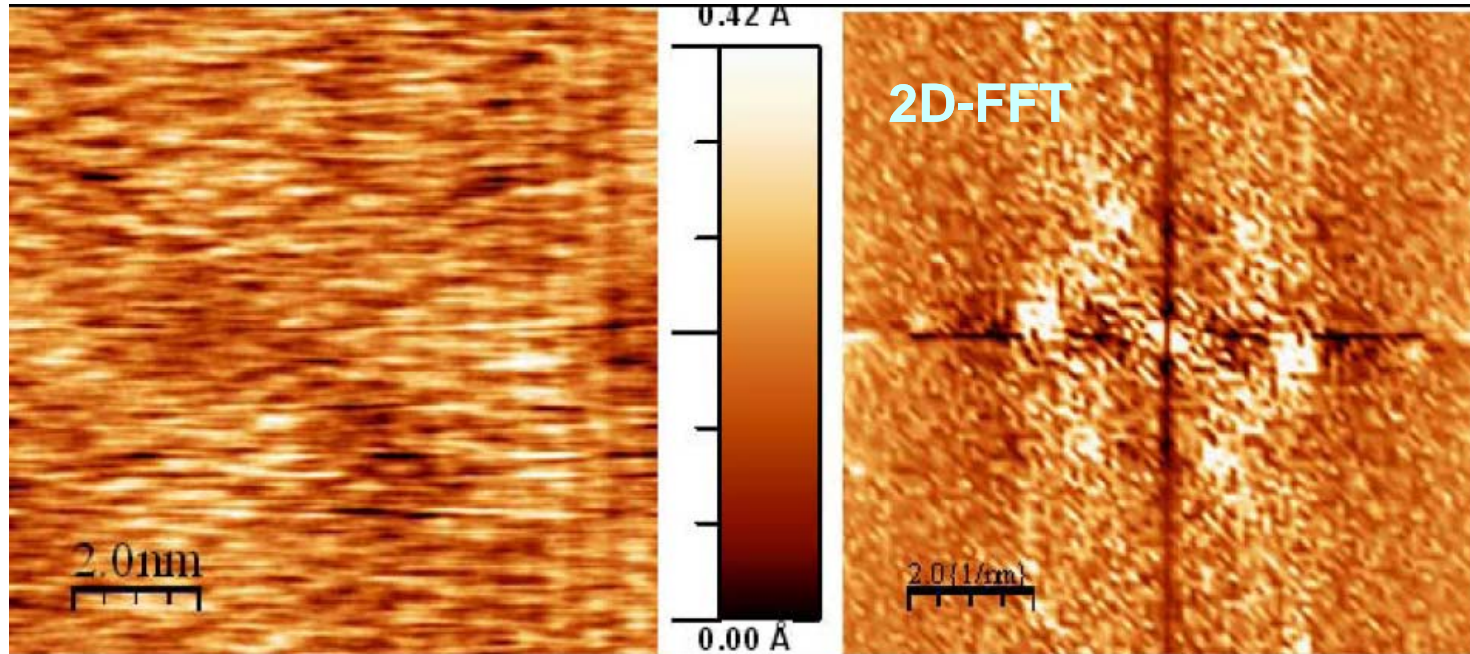
A butterfly (*Gynnisone celeris*) wing imaged in tappingmode AFM. The well ordered 3-D lattice is an array of holes on the cuticle of the scales. The order of such a system leads to strong diffraction of favored wavelengths in certain directions. This scattering process and pigmentation causes the coloration of the butterfly. 6.25 μ m scan courtesy of J. Wuest, Museum d'Histoire Naturelle, Switzerland.



The sample is a strip of adhesive (3M Scotch tape) that has been peeled of a metal surface. The image shows small pits in the sticky surfaces of the adhesive. The image was acquired in TappingMode at frequency of 3 Hz and setpoint of 1.8 V. 2 μ m scan courtesy L. Scudiero, Washington State University, USA.

Huge variety of AFM applications!!

A very few examples of AFM images III



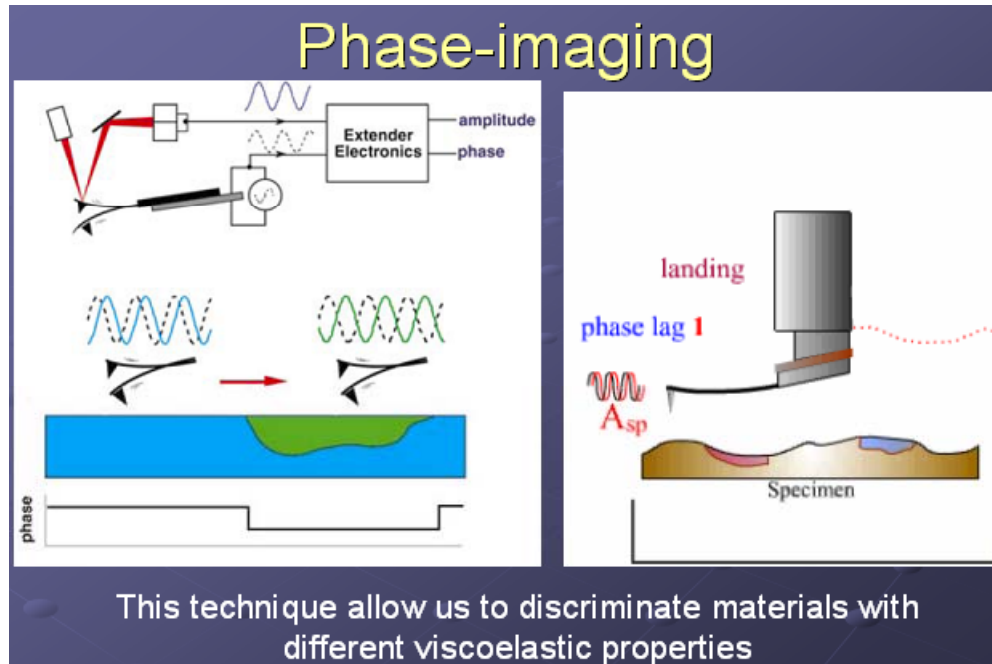
Contact-mode topography of
nonanethiol SAM grown on
Au/mica

Hexagonal arrangement
→ structural variant

$$c(\sqrt{3} \times \sqrt{3})R30^\circ$$

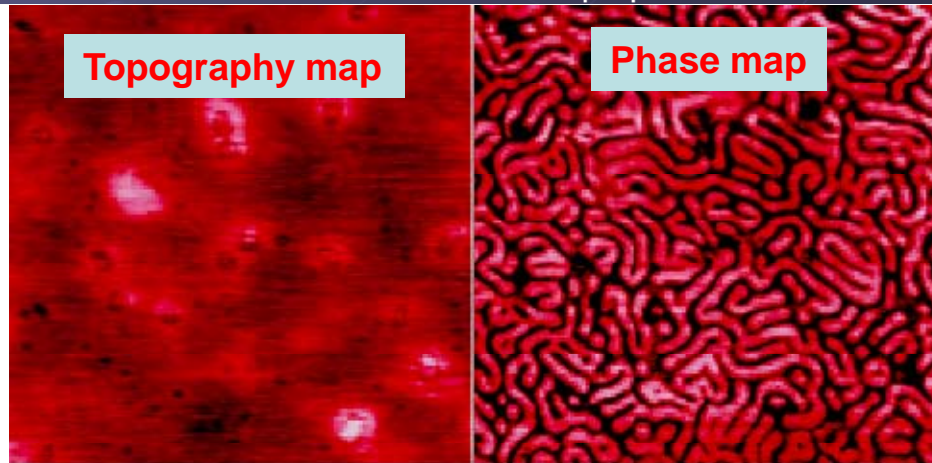
Phase imaging techniques

Animations at www.ntmdt.com!



Dephasing between mechanical oscillation (e.g., the tapping oscillation) and the response of the surface (affecting the tip deflection) depends on the viscoelasticity of the surface (purely elastic vs Newton fluid)

Interpretation similar to a forced and damped mechanical oscillator



Phase imaging:
- adds a contrast mechanism;
- allows for local material analyses

Materiale tratto da seminario PhD di Michele Alderighi, 2005

4.A. Nanoindentation and AFM

Introduction to nanoindentation

<http://www.nanoindentation.cornell.edu/>

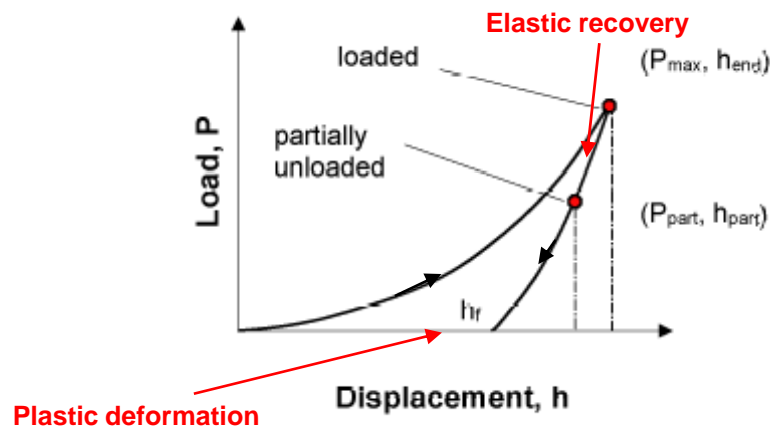
Indentation tests are perhaps the most commonly applied means of testing the mechanical properties of materials. In such a test, a hard tip, typically a diamond, is pressed into the sample with a known load. After some time, the load is removed. The area of the residual indentation in the sample is measured and the hardness, H , is defined as the maximum load, P , divided by the residual indentation area, A_r , or

$$H = P/A_r$$

The idea of nanoindentation arose from the realization that an indentation test is an excellent way to measure very small volumes of materials. In principle, if a very sharp tip is used, the contact area between the sample and the tip, and thus the volume of material that is tested, can be made arbitrarily small. The only problem is determining the indentation area. It is easy to make an indentation that is so small that it is difficult to see without a powerful microscope.

To solve this problem depth sensing indentation methods were developed. In this method, the load and displacement of the indenter are recorded during the indentation process and these data are analyzed to obtain the contact area, and thereby mechanical properties, without having to see the indentations.

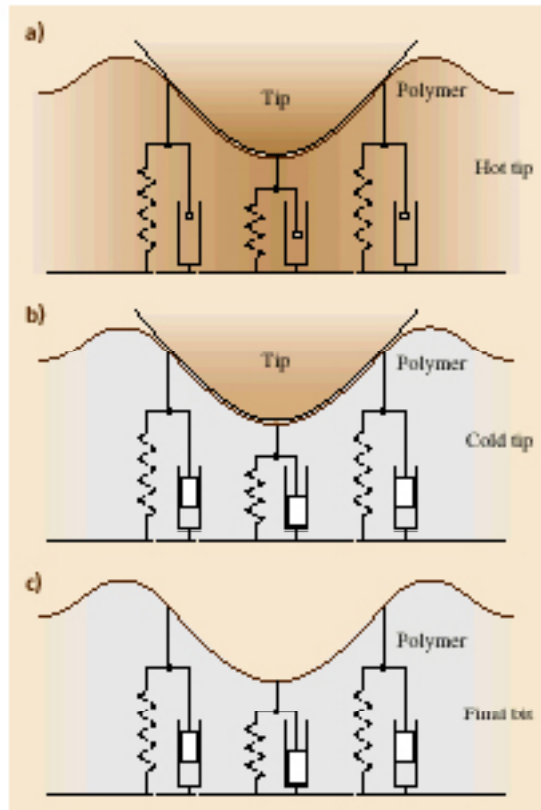
Nanoindentation refers to depth-sensing indentation testing in the submicrometer range and has been made possible by the development of 1) machines that can make such tiny indentations while recording load and displacement with very high accuracy and precision, and 2) analysis models by which the load displacement data can be interpreted to obtain hardness, modulus, and other mechanical properties.



(Nano)indentation is a common technique to ascertain elastic/plastic behavior of the materials (if carried out with a load modulation, also surface viscoelasticity can be analyzed)

Data pertaining to the elastic modulus and to the plastic behavior (e.g., shear modulus) can be attained and comparison with macroscopic results (e.g., Vickers hardness, Rockwell,...) may lead to interesting insights on the microscopic nature of surfaces and nanostructures

More details on nanoindentation



31.7 Polymer Medium

The polymer storage medium plays a crucial role in millipede-like thermomechanical storage systems. The thin-film multilayer structure with PMMA as active layer (see Fig. 31.2) is not the only possible choice, considering the almost unlimited range of polymer materials available. The ideal medium should be easily deformable for writing, yet indentations should be stable against tip wear and thermal degradation. Finally, one would also like to be able to erase and rewrite data repeatedly. In or-

Polymers can be plastically deformed

If thermoplastics are used (and tip is heated), deformations can be reversed

Fig. 31.18a–c viscoelastic model of indentation writing. (a) The hot tip heats a small volume of polymer material to more than Θ_g . The shear modulus of the polymer drops drastically from GPa to MPa, which in turn allows the tip to indent the polymer. In response, elastic stress (represented as compression springs) builds up in the polymer. In addition, viscous forces (represented as pistons) associated with the relaxation time for the local deformation of molecular segments limit the indentation speed. (b) At the end of the writing process, the temperature is quenched on a microsecond time scale to room temperature: The stressed configuration of the polymer is frozen-in (represented by the locked pistons). (c) The final indentation corresponds to a metastable configuration. The original unstressed flat state of the polymer can be recovered by heating the indentation volume to more than Θ_g , which unlocks the compressed springs (after [31.15])

der to be able to address all important aspects properly, some understanding of the basic physical mechanism of thermomechanical writing and erasing is required.

31.7.1 Writing Mechanism

In a *gedanken* experiment we visualize writing of an indentation as the motion of a rigid body (the tip) in a viscous medium (the polymer melt). Let us initially assume

that the polymer, i. e., PMMA, behaves like a simple liquid after it has been heated above the glass-transition temperature in a small volume around the tip. As viscous drag forces must not exceed the loading force applied to the tip during indentation, we can estimate an upper bound for the viscosity ζ of the polymer melt using Stokes's equation:

$$F = 6\pi\zeta\dot{v}r \quad (31.1)$$

In actual indentation formation, the tip loading force is on the order of $F = 50 \text{ nN}$ and the radius of curvature at the apex of the tip is typically $r = 20 \text{ nm}$. Assuming a depth of the indentation of, say, $h = 50 \text{ nm}$ and a heat pulse of $\tau_0 = 10 \text{ }\mu\text{s}$ duration, the mean velocity during indentation formation is on the order of $v = h/\tau_0 = 5 \text{ mm/s}$. Note that thermal relaxation times are on the order of microseconds [31.20, 21] and, hence, the heating time can be equated to the time it takes to form an indentation. With these parameters we obtain $\zeta < 25 \text{ Pa}\cdot\text{s}$, whereas typical values for the shear viscosity of PMMA are at least seven orders of magnitude larger even at temperatures well above the glass-transition point [31.39].

This apparent contradiction can be resolved by considering that polymer properties are strongly dependent on the time scale of observation. At time scales on the order of 1 ms and below, entanglement motion is in effect frozen in and the PMMA molecules form a relatively static network. Deformation of the PMMA now proceeds by means of uncorrelated deformations of short molecular segments, rather than by a flow mechanism involving the coordinated motion of entire molecular chains. The price one has to pay is that elastic stress builds up in the molecular network as a result of the deformation (the polymer is in a so-called rubbery state). On the other hand, corresponding relaxation times are orders of magnitude smaller, giving rise to an effective viscosity at millipede time scales on the order of 10 Pa·s [31.39], as required by our simple argument (see (31.1)). Note that, unlike normal viscosity, this high-frequency viscosity is basically independent of the detailed molecular structure of the PMMA, i. e., chain length, tacticity, polydispersity, etc. In fact, we can even expect that similar high-frequency viscous properties can be found in a large class of other polymer materials, which makes thermomechanical writing a rather robust process in terms of material selection.

Examples of nanoindentation I

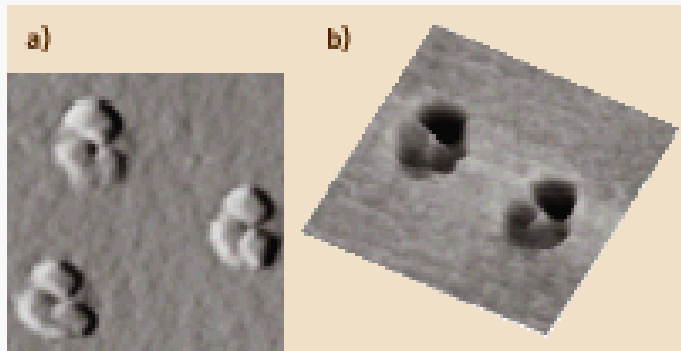


Fig. 31.20a,b Topographic image of individual indentations. (a) The region around the actual indentations clearly shows the threefold symmetry of the tip, here a three-sided pyramid. (b) The indentations themselves exhibit sharp edges, as can be seen from the inverted 3-D image. Image size is $2 \times 2 \mu\text{m}^2$ (from [31.15] © 2002 IEEE)

Besides tribological and nanomechanical applications, nanoindentation can be envisioned as a nanofabrication tool or a data storage method

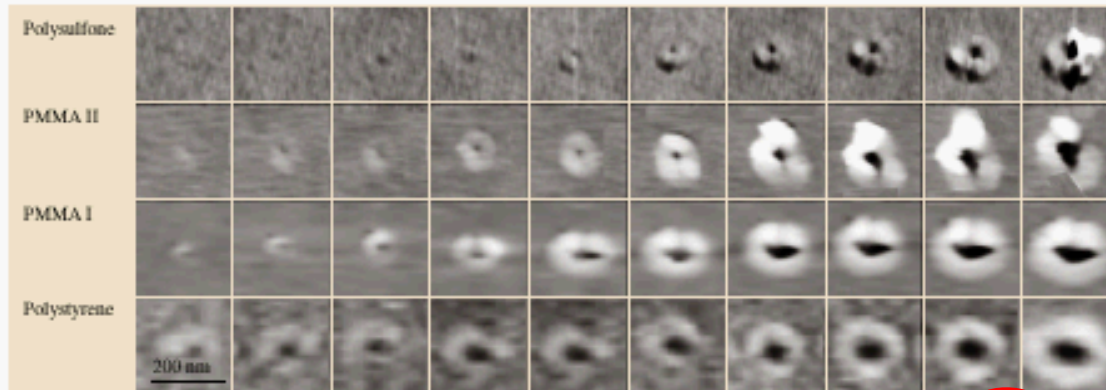


Fig. 31.21 Written indentations for different polymer materials. The heating pulse length was $10 \mu\text{s}$, the load about 10 nN . The grey scale is the same for all images. The heater temperatures for the indentation on the left-hand side are 445, 400, 365, and 275°C for the polymers Polysulfone, PMMA II (anionically polymerized PMMA, $M \approx 26 \text{ k}$), PMMA I (Polymer Standard Service, Germany, $M \approx 500 \text{ k}$), and Polystyrene, respectively. The temperature increase between events on the horizontal axis is 14, 22, 20, and 9°C , respectively (from [31.15] © 2002 IEEE)

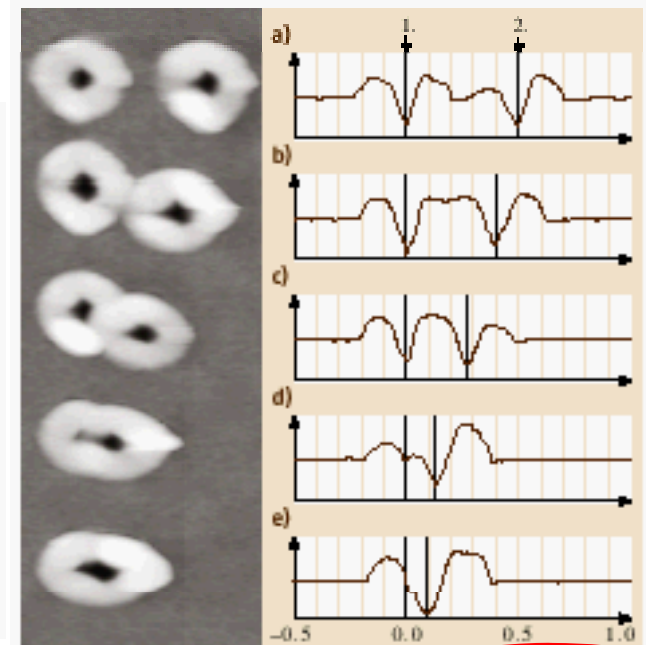


Fig. 31.24a-e Indentations in a PMMA film at several distances. The depth of the indentations is $\sim 15 \text{ nm}$, roughly the same as the thickness of the PMMA layer. The indentations on the left-hand side were written first, then a second series of indentations was made with decreasing distance from the first series going from (a) to (e) (after [31.15])

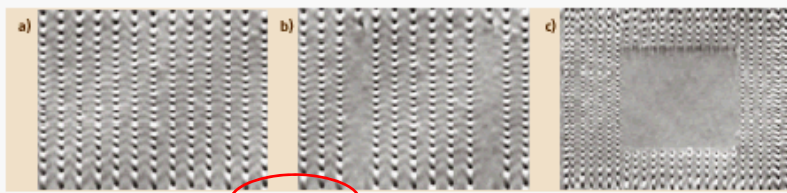
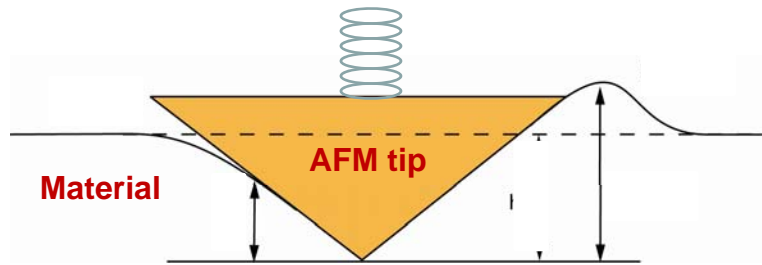


Fig. 31.25a-c Demonstration of the new erasing scheme. (a) A bit pattern recorded with variable pitch in the vertical axis (fast scan axis) and constant pitch in the horizontal direction (slow scan axis) was prepared. (b) Then two of the lines were erased by decreasing the pitch in the vertical direction by a factor of three, showing that the erasing scheme works for individual lines. One can also erase entire fields of indentations without destroying indentations at the edges of the fields. This is demonstrated in (c), where a field has been erased from an indentation field similar to the one shown in (a). The distance between the lines is 70 nm (from [31.15] © 2002 IEEE)

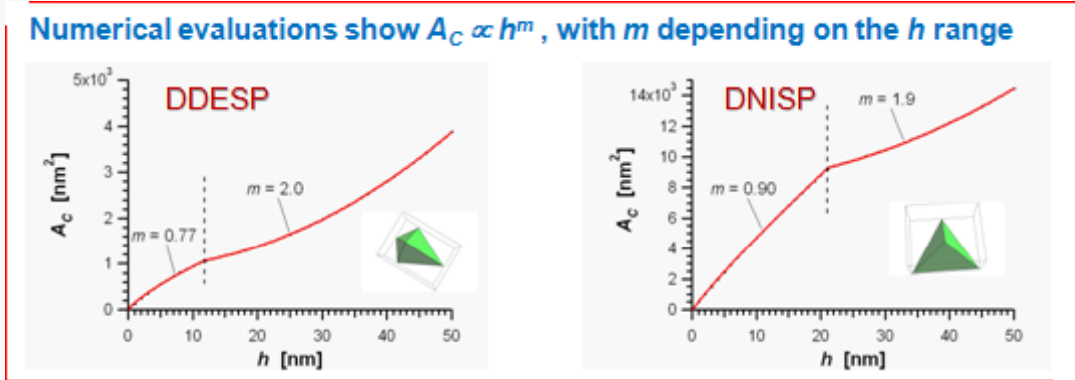
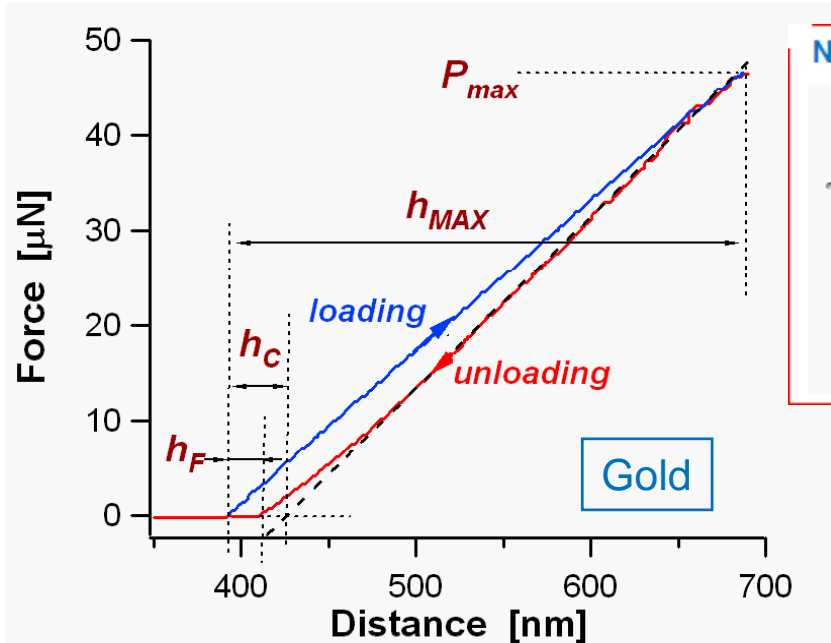
Da B. Bhushan, Handbook of nanotechnology (Springer, 2003)

Examples of nanoindentation II



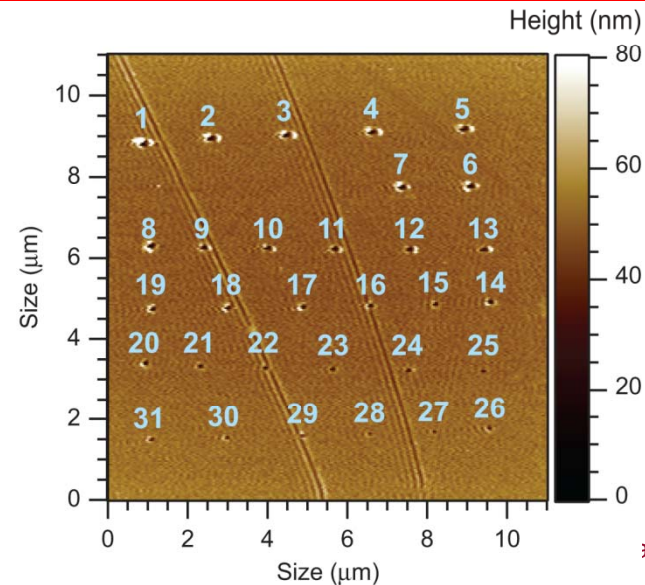
Material hardness:

$$H = \frac{P_{MAX}}{A_C}$$



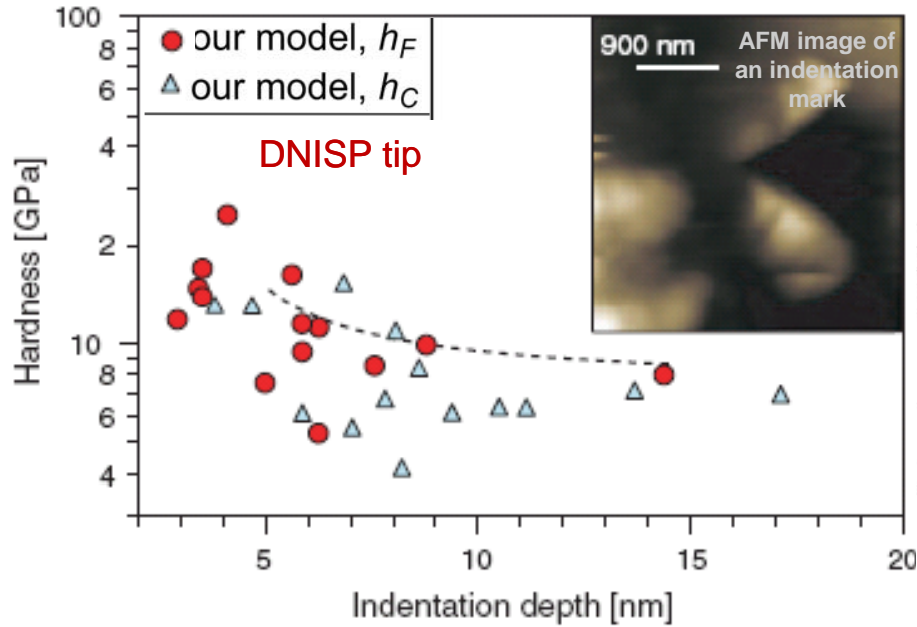
Either h_F or h_C can be used as representative of the indentation depth h

Contact area derived from h through specific models



Examples of nanoindentation III

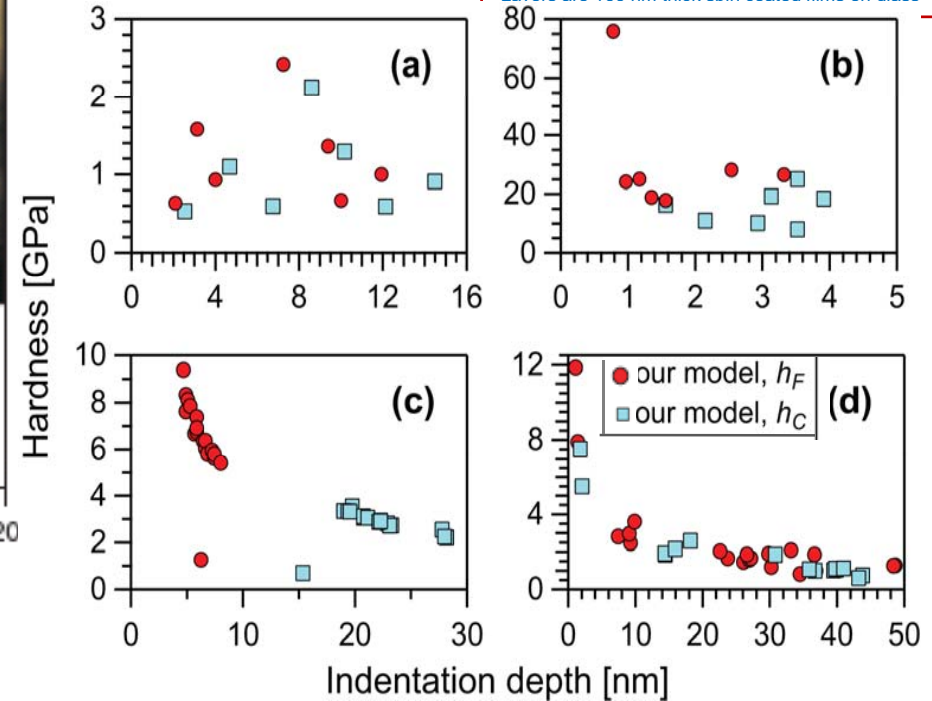
Nanoindentation of a hard coating (BALINIT C)



Material	Investigated depth range [nm]	α	H_0 [GPa]	Literature data [GPa]
Silicon	0.5-4.0	-1.9	13±2.4	13
Gold	5-28	-1.3	1.3±0.2	1.1-1.4
Balinit C	2-15	-1.0	5.5±1.2	5-8 (?)
Polystyrene	3.0-10	-1.2	0.83±0.2 2	~0.3
PMMA	1.0-30	-0.73	0.58±0.1 6	~0.4

- (a) Aluminium Bulk DNISP
- (b) Silicon Wafer DNISP
- (c) Polystyrene Layer DDESP
- (d) PMMA Layer DDESP

Layers are 100 nm thick spin coated films on glass



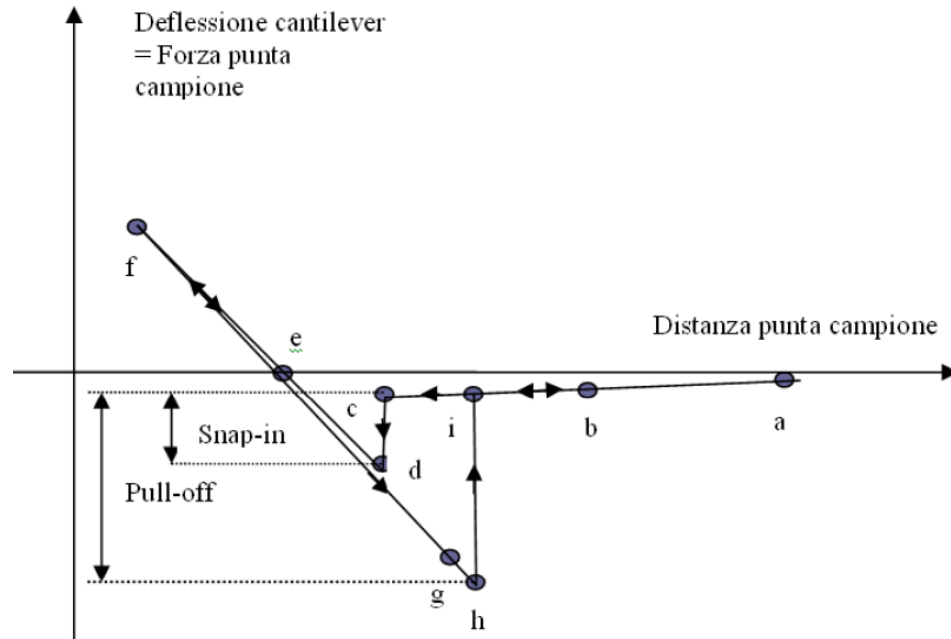
Behavior of H on h_F :

$$H(h_F) = kh_F^\alpha + H_0$$

with k constant, $\alpha < 0$,
 H_0 asymptotic hardness at macroscopic indentations

(Apparent) hardness increase at small (<10 nm) indentation depths

Measurement of adhesion forces



Oro: adesione = (19 ± 1) nN
 SAM: adesione = (5.5 ± 0.3) nN

SAM < ORO perché ha superficie idrofobica

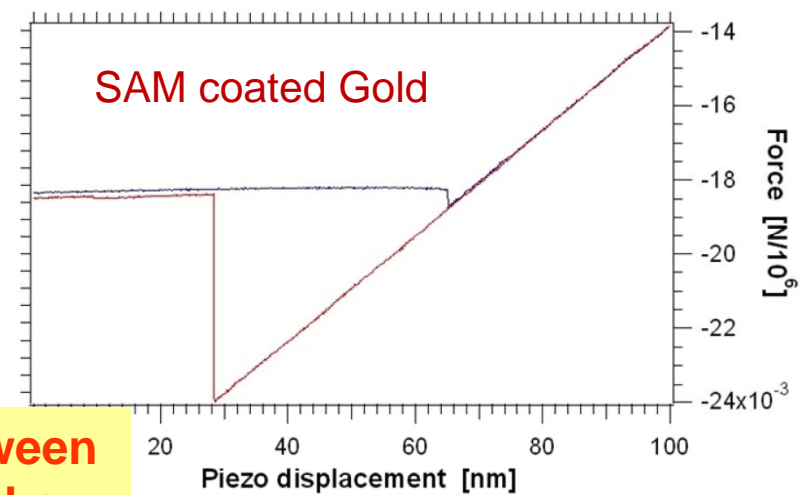
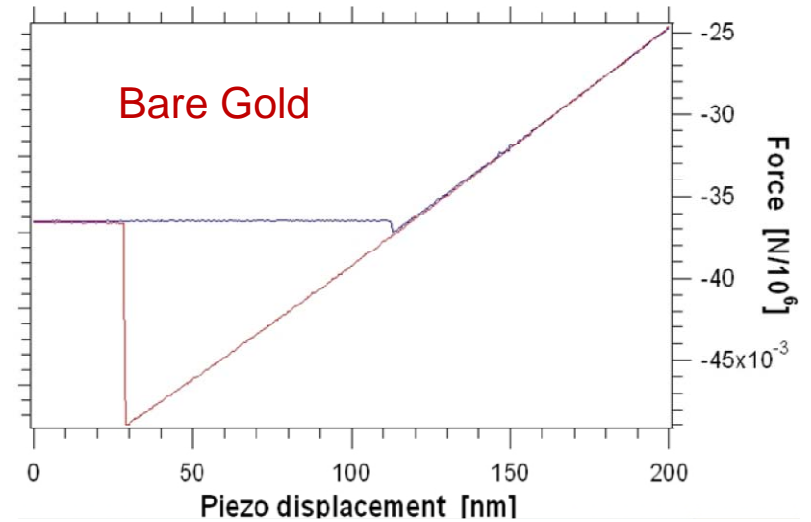
Lavoro adesione SAM per unità di superficie = 44 mJ/m^2

Molecola SAM = piccola molla

$k \text{ molecola} = 3 \text{ N/m}$

Adhesion forces of SAM (nonanethiol) layers

Adhesion forces between tip and surface can be accurately measured



F. Prescimone, Tesi di laurea in Scienza dei Materiali, 2008

2.B. Force microscopies derived from AFM

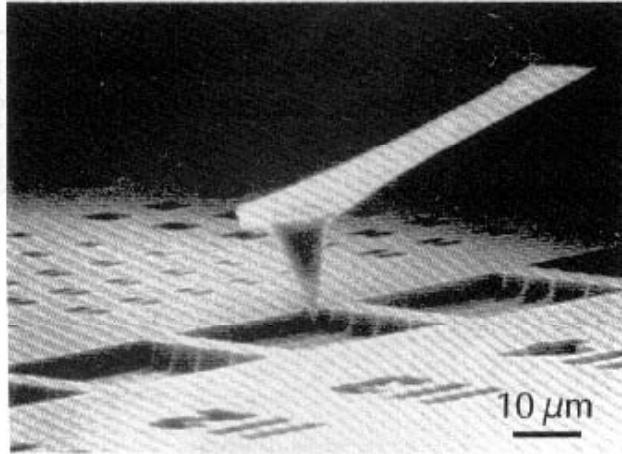


Figure 19: Scanning electron micrograph of a cantilever made of Si. [24].

We have seen how AFM, based on the occurrence of tip/surface van der Waals forces, can map the local topography of the sample

No sample preparation is needed, and the topography map is obtained with “absolute” calibration

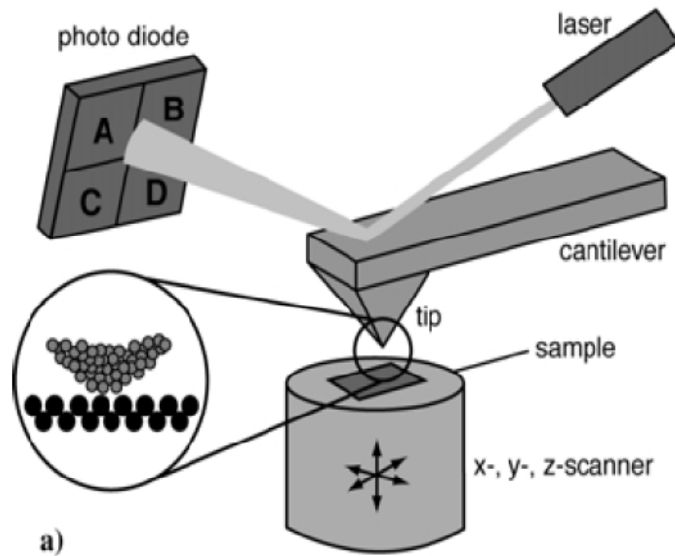
The achievable space resolution can reach the **atomic level**, even though most common instruments are capable of a slightly smaller resolution (in the nm range, depending also on the sample properties!)

The close vicinity between tip and surface realized in AFM opens the way for probing physical **quantities other** than the van der Waals interaction force

For instance, tribological and material quantities can be measured (e.g., friction, viscoelasticity, Young modulus, etc.)

With suitable tips (conductive, magnetic), static and quasi-static electromagnetic forces locally occurring at the sample surface can be analyzed

Lateral Force Microscopy (LFM, SFFM)

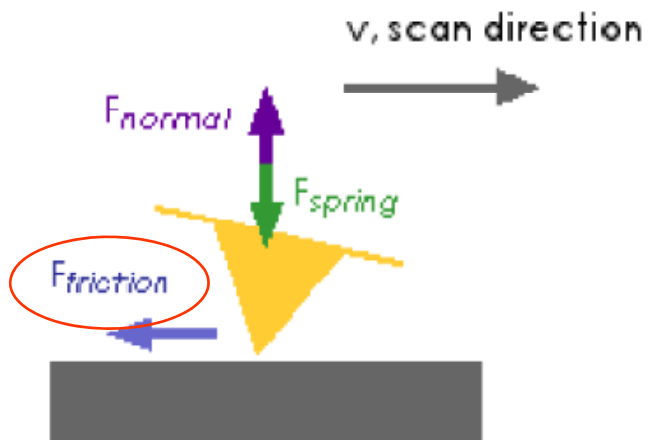


During the scan, the tip is continuously displaced with respect to the surface

Friction forces occur, resulting in a *twisting* of the cantilever

Cantilever twist can be recorded by a two-dimension position sensitive detector (i.e., a 4-quadrant photodetector)

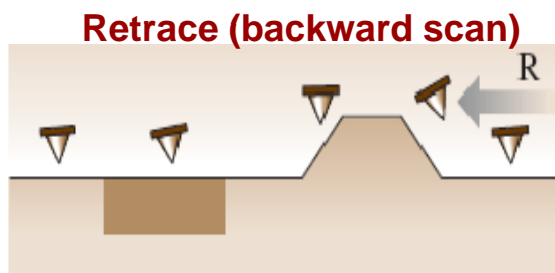
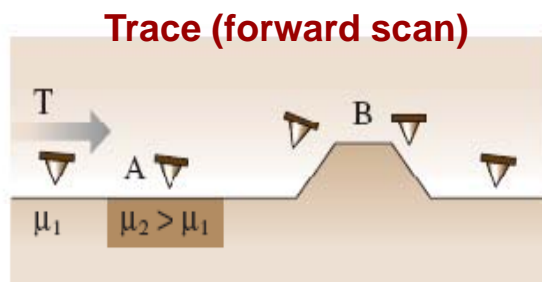
Friction effects can be corrected by the topographical artifacts by comparing forward and backward scans



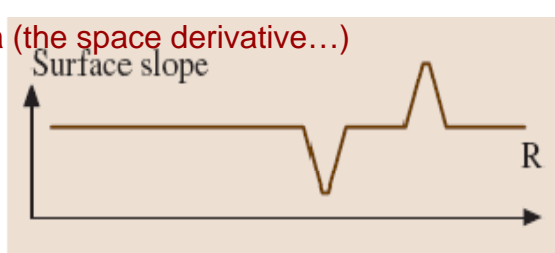
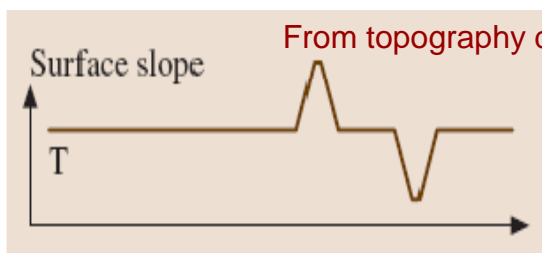
- $(A+B)-(C+D)$ = normal force (AFM signal)
- $(A+C)-(B+D)$ = lateral force (LFM signal)

Materiale tratto dal seminario di Cinzia Rotella, 2006

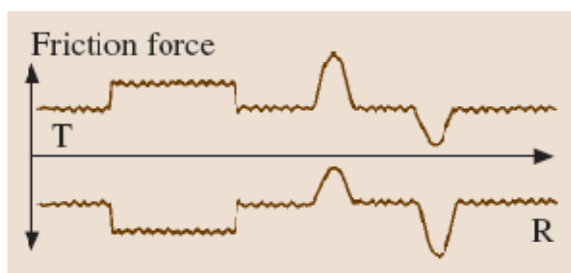
Friction and topography: artifacts and genuine



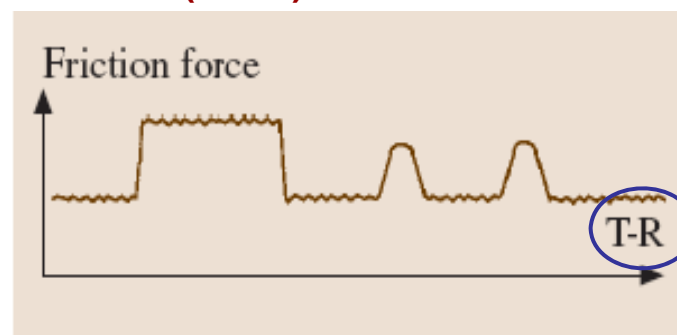
Friction force is **always** oriented against motion!



Lateral force data



(Local) friction data



Lateral force data are always convoluted with topography (slope), but genuine information of the local friction can be derived by comparing trace and retrace and considering simultaneously acquired topography data

nanotechnology (Springer, 2003)

Examples of LFM/SFFM images

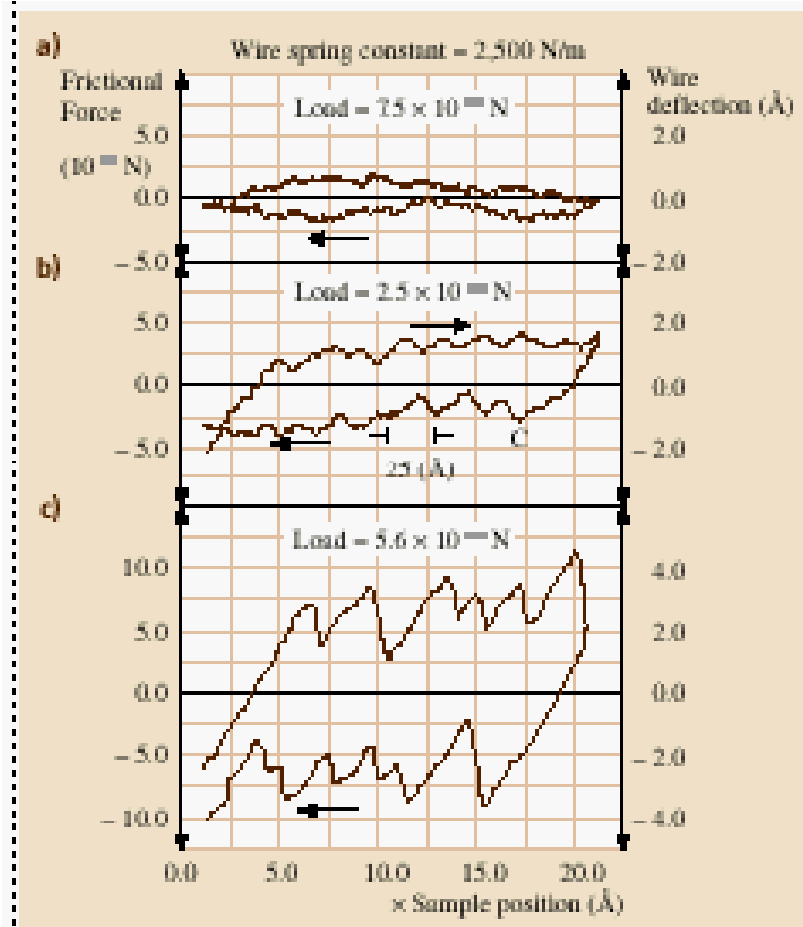


Fig. 20.15a-c Friction loops on graphite acquired with (a) $F_N = 7.5 \mu\text{N}$, (b) $24 \mu\text{N}$ and (c) $75 \mu\text{N}$. (After [20.1])

- ✓ LFM/SFFM offers an additional contrast mechanism
- ✓ Possibility to discriminate different materials at the atom level
- ✓ Nanotribology investigations can be carried out

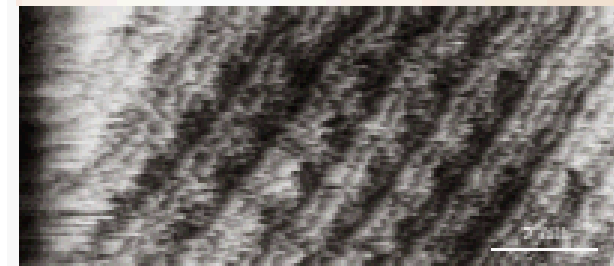


Fig. 20.18 (a) Topography and (b) friction image of Si(111)7x7 measured with a PTFE coated Si-tip. (After [20.29])

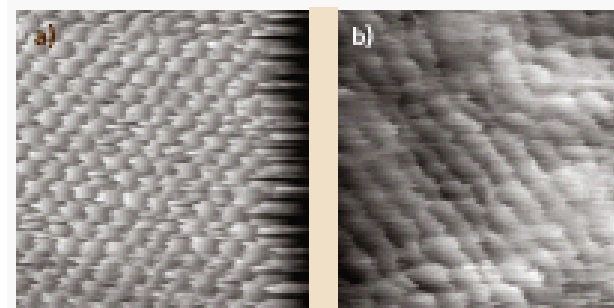
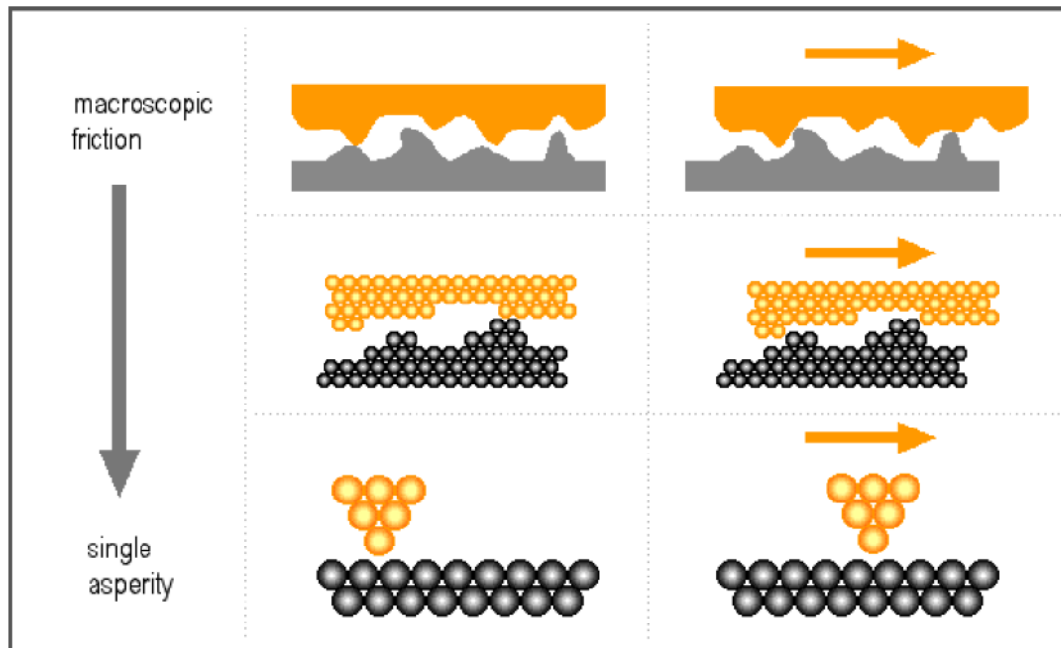


Fig. 20.19a,b Friction images of (a) Ca(111) and (b) Ca(100). Frame size: 3 nm. (After [20.34])

Da B. Bhushan, Handbook of nanotechnology (Springer, 2003)

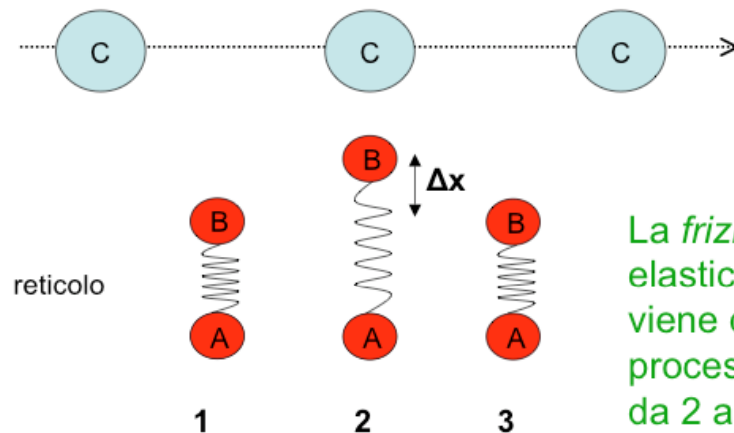
A few words on nanotribology



Sliding motion of the AFM tip “in contact” with the surface turns out affected by “tribological mechanisms” at the atomic scale:

- **Adhesion;**
- **Ploughing;**
- **Deformation**

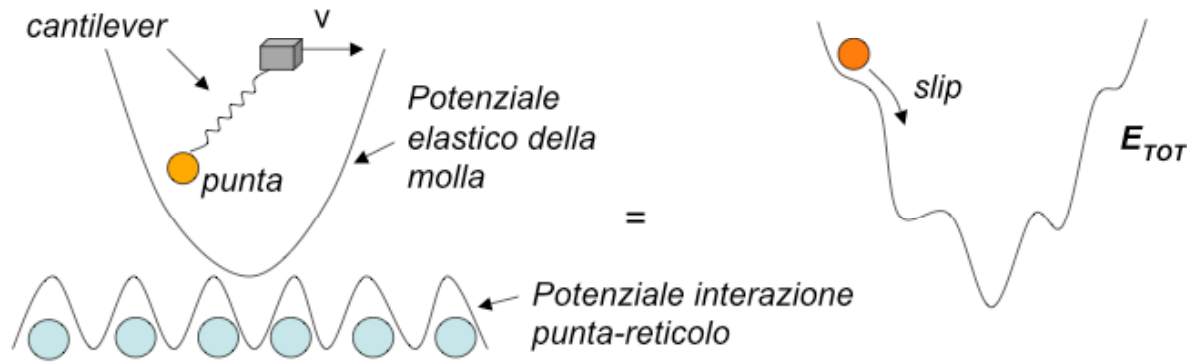
- Modello di Tomlinson (1929) :
modello di attrito applicabile su scala atomica



La *frizione* è l'energia elastica $\frac{1}{2} K(\Delta x)^2$ che viene dissipata nel processo di rilassamento da 2 a 3

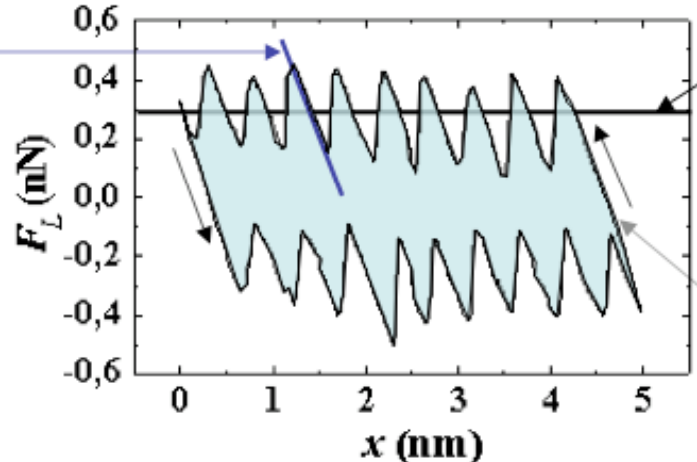
Friction models at the atomic scale must account for local tip /surface interaction

Stick-slip mechanism during the scan



Interaction potential accounts for the periodic surface potential

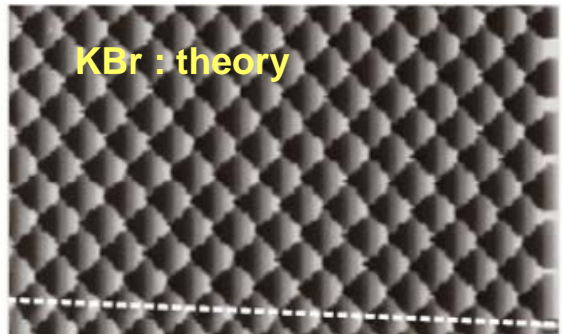
Pendenza nella regione di equilibrio:
costante elastica che rappresenta le interazioni punta-campione
 $1/K_{\text{eff}} = 1/K_T + 1/K_C$



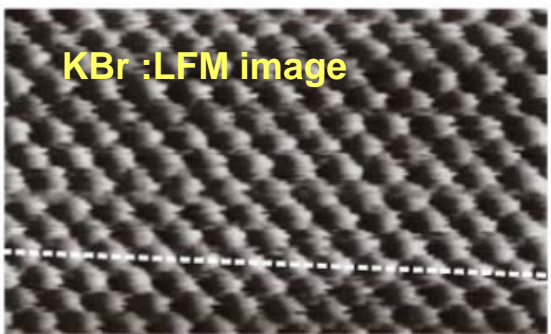
Forza laterale media:
permette il calcolo di μ

Area dentro il ciclo di isteresi: energia totale dissipata

Singola linea di scansione LFM di NaCl a $v = 2.5 \text{ nm/s}$



KBr : theory



KBr : LFM image

Detailed and quantitative info can be achieved at the atomic level

Magnetic Force Microscopy (MFM)

3.3.2 Magnetic Scanning Force Microscopy (MFM)

If a magnetic tip is used in the scanning force microscope, magnetic structures can be imaged. Magnetic scanning force microscopy is of interest, in particular, for the investigation of magnetic storage media. In the most general case, the magnetic force between sample and tip is

$$F_{\text{mag}} = -\nabla \int_{\text{tip}} \mathbf{M}_{\text{tip}} \cdot \mathbf{H}_{\text{sample}} dV \quad (13)$$

or

$$F_{\text{mag}} = (\mathbf{m}_{\text{tip}} \nabla) \mathbf{B}_{\text{sample}} \quad (14)$$

where $\mathbf{H}_{\text{sample}}$ and $\mathbf{B}_{\text{sample}}$ are the magnetic stray field and the magnetic induction of the sample, respectively. \mathbf{M}_{tip} and \mathbf{m}_{tip} are the magnetisation and the magnetic moment of the tip, respectively. Since in most cases the exact magnetic structure of the tip is not known, a model tip magnetization must be assumed. In the simplest case, the tip is a spherically structured magnetic single domain with the magnetisation \mathbf{M}_{tip} . Of particular interest are the stray fields of magnetic storage media which consist of different domains. Since the important aspect in force microscopy is not the forces but the force gradient, a pronounced variation of the signal is found near the domain walls, but not inside a domain. This situation is sketched in Figure 21. The parameter of the two curves shown (solid and broken lines) is the ratio of the working distance d and the radius R of the magnetic domain of the tip.

Figure 22a shows an experimentally measured picture of four different oriented magnetic domains. Images b and c show the fine structure of a 180° domain. Alternating bright and dark contrasts can be seen. These contrast changes show that the domain wall consists of segments with different wall orientation. This example illustrates that magnetic SFM is well suited for imaging magnetic structures that are commonly used in today's storage media.

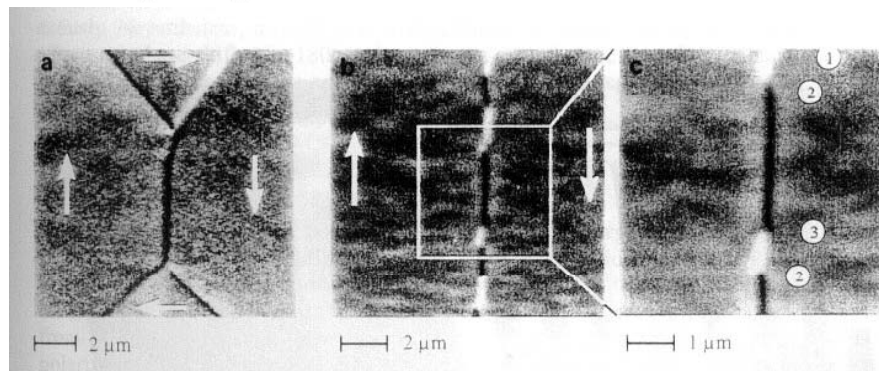


Figure 22: Magnetic SFM image of magnetic domains. (a) shows four domains of a Landau-Lifshitz structure in which the domain walls are the dark and bright lines. (b) and (c) show the fine structure of a 180° domain wall. The domain wall consists of segments with different wall orientation. Arrows denote the domain orientation. (after [26]).

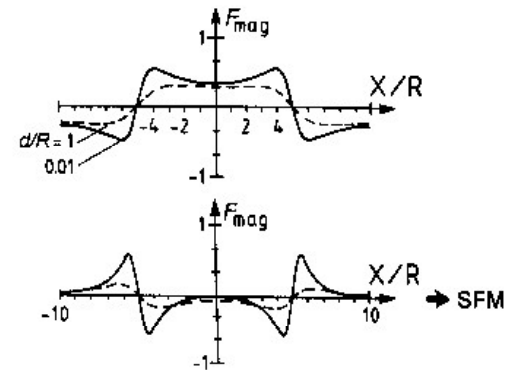
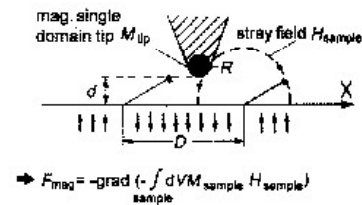


Figure 21: Principle of magnetic scanning force microscopy. On the left, the tip-sample configuration is shown and on the right the force and nominal force constant as a function of distance for this configuration. Two domain walls exist at position 5 (after [23]).

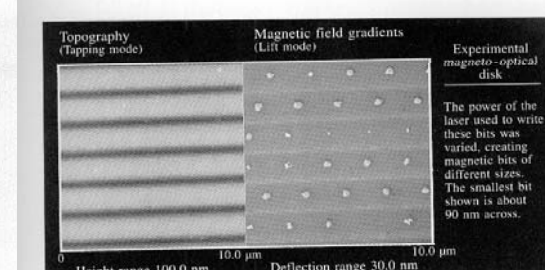


Fig. 5.21. A pair of images of a magneto-optical disk [5.36]

Electrostatic Force Microscopy (EFM)

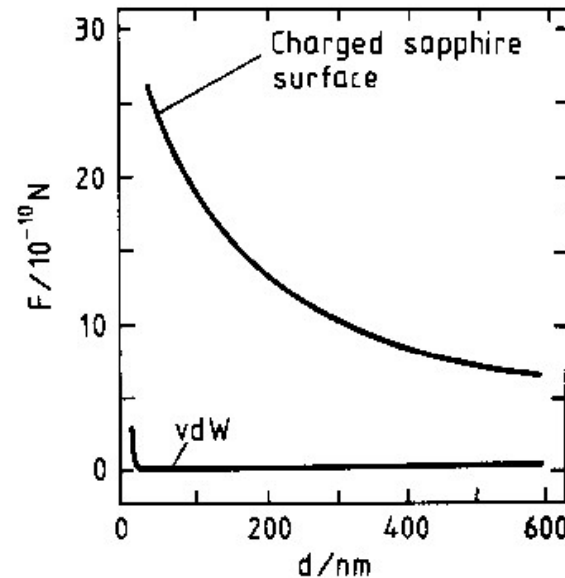
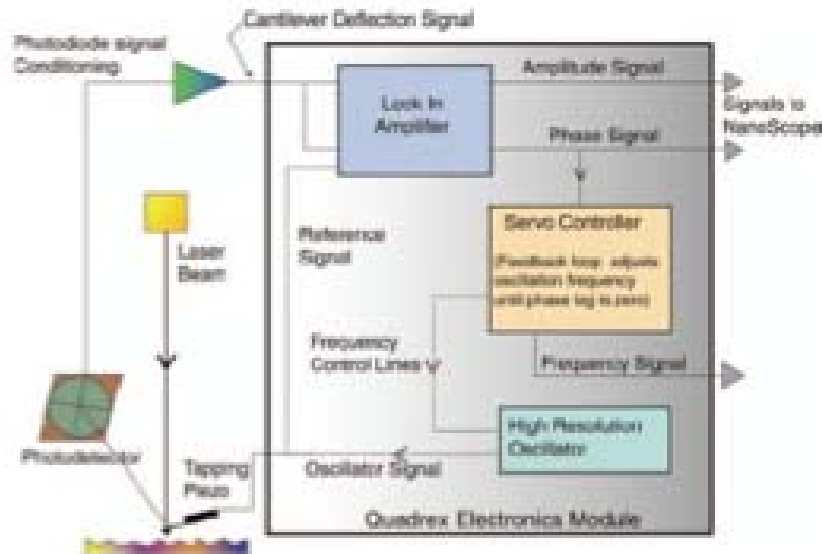


Figure 26: Comparison of the distance dependence of the electrical and van der Waals forces between a tip and a local electrical surface charge of $2 \cdot 10^{-16} \text{ C}$ (after [23]).

Basic idea: application of a ddp between tip at sample in order to be sensitive to electric forces, thus to the space distribution of charges on the sample surface and to its electrostatic potential

Modulation/demodulation techniques used to get direct information on various surface/tip interaction features

Excellent sensitivity to local charges

Application to electronic devices (also in operating conditions)

Application to ferroelectric materials (also known as Piezoelectric Force Microscopy - PFM)

Operating modes in EFM

- Un EFM viene utilizzato principalmente per misurare il potenziale elettrostatico locale della superficie. A tale scopo alla punta viene applicata esternamente una tensione con una componente continua V_{dc} e una componente V_{ac} modulata alla frequenza Ω . Il campione è invece collegato a massa. La forza elettrostatica tra punta e campione è data da [1]:

$$F = \frac{1}{2} \frac{dC}{dz} V^2$$

C rappresenta l'accoppiamento capacitivo tra punta e campione mentre z è la variabile che indica la quota della punta. In V compaiono la tensione applicata ($V_{dc} + V_{ac} \sin(\Omega t)$) una eventuale tensione indotta sulla punta da altri effetti secondari (V_{ind}) e la tensione locale del campione (V_{cp}).

$$V = (V_{cp} + V_{dc} + V_{ind}) + V_{ac} \sin(\Omega t)$$

La forza elettrostatica tra il campione e la punta può essere scomposta in tre componenti a frequenze diverse:

$$F = \frac{1}{2} \frac{dC}{dz} V^2 = \frac{1}{2} \frac{dC}{dz} [(V_{cp} + V_{dc} + V_{ind}) + V_{ac} \sin(\Omega t)]^2 = F_{dc} + F_{\Omega} + F_{2\Omega}$$

Esaminiamo ora in dettaglio le tre componenti.

- Il primo termine della forza è costante nel tempo ed è pari a:

$$F_{dc} = \frac{1}{2} \frac{dC}{dz} [(V_{cp} + V_{dc} + V_{ind})^2 + \frac{1}{2} V_{ac}^2]$$

- Il secondo termine invece dipende direttamente dalle quantità di interesse come dC/dz o $(V_{cp} + V_{ind})$ ed è modulato alla frequenza Ω :

$$F_{\Omega} = \frac{dC}{dz} (V_{cp} + V_{dc} + V_{ind}) V_{ac} \sin(\Omega t)$$

- Il terzo termine è modulato alla frequenza 2Ω ed è molto importante perché dipende esclusivamente da V_{ac} , che è noto, e da dC/dz :

$$F_{2\Omega} = -\frac{1}{4} \frac{dC}{dz} V_{ac}^2 \cos(2\Omega t)$$

Materiale tratto dal seminario di Nicola Paradiso, 2006

Operazione in modalità nano-Kelvin

Come si è detto precedentemente operando con un EFM occorre fornire una tensione con una componente continua e una modulata. Se con un circuito di reazione noi iniettiamo una tensione V_{dc} tale che il termine $F_{dc} = 0$, per cui $V_{dc} = -(V_{cp} + V_{ind})$, allora potremo misurare variazioni di tensione sulla superficie dovute a sia a V_{cp} che a V_{ind} .

Impiego di un EFM per misure in dc

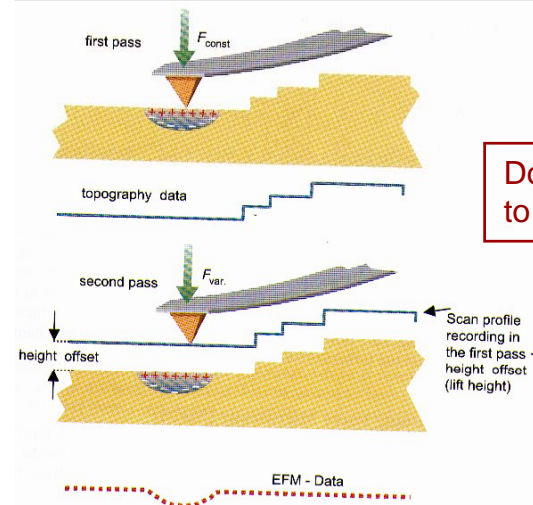
L'utilizzo dell'EFM è basato sull'assunto che la forza elettrostatica sia un effetto al secondo ordine sull'oscillazione meccanica [1]. Tali effetti vengono separati per mezzo di due amplificatori lock-in che permettono di estrarre il segnale modulato alla frequenza Ω e quello alla frequenza 2Ω . E' conveniente scegliere la frequenza Ω in modo da lavorare lontani dalla risonanza di oscillazione meccanica. Come si è detto, conviene inserire anche un circuito di reazione per poter misurare e mappare il potenziale elettrico superficiale. Queste operazioni richiedono che la distanza punta-campione sia stabile durante la misura. Esaminiamo brevemente due metodi che permettono di lavorare in tali condizioni.

Modalità single-pass

Operando in aria, l'ampiezza dell'oscillazione meccanica della cantilever vicina alla risonanza è in genere debolmente dipendente da eventuali interazioni elettrostatiche. Se però localmente i valori di V_{cp} e di V_{ind} diventano molto intensi l'immagine topografica che si ricava può risultare disturbata. In modalità single-pass si utilizzano tensioni dc basse e si acquisiscono simultaneamente i dati sulla topografia (ottenuti facendo oscillare la sonda in tapping mode), i dati del segnale alla frequenza Ω e alla frequenza 2Ω . Operando in modalità nano-Kelvin in pratica si sottrae la tensione V_{cp} che disturba l'immagine, mentre con il segnale alla frequenza 2Ω si ricava il valore dell'accoppiamento capacitivo locale.

Modalità double-pass

Questa modalità prevede un primo passaggio volto ad acquisire il profilo topografico locale. La cantilever viene posta in oscillazione (tapping mode) senza che le venga applicata alcuna tensione esterna. Alla fine della scansione della linea, il piezo si ritira, allontana la sonda dal campione di una certa quantità fissata e riprende la scansione nel senso opposto, mantenendo fissa la quota basandosi sui dati topografici appena acquisiti. In questa fase la punta è relativamente più sensibile alle forze elettrostatiche in quanto forze a lungo range. Nello specifico qui viene rilevata la variazione di fase dovuta al gradiente di forza elettrostatica. Rispetto alla modalità single-pass questa modalità ha il vantaggio di essere più sensibile alle proprietà elettrostatiche del sistema. Lo svantaggio è rappresentato dalla perdita di risoluzione dovuta all'aver aumentato la quota di lavoro.



Double-pass technique to get rid of topography

Examples of EFM images

Electronic devices

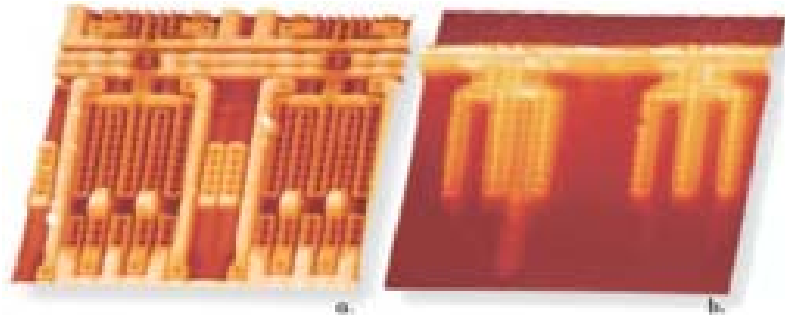


Figure 6. Topography (a) and EFM image (b) of a live packaged IC with passivation layer on. EFM image detects transistor in saturation. 80µm scans.

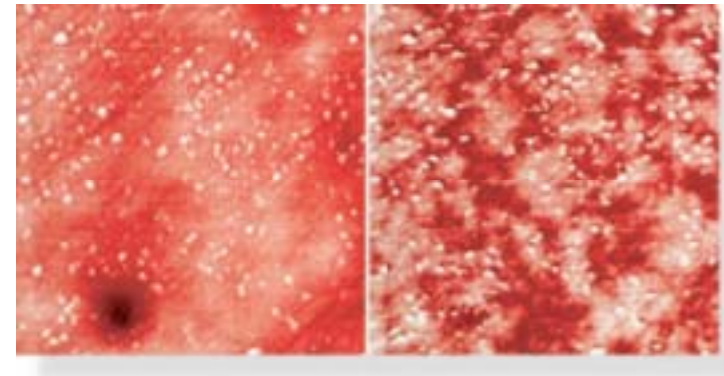
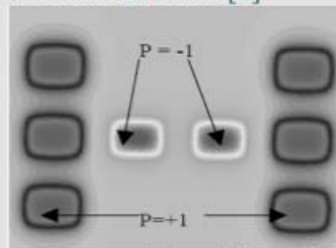


Figure 11. Topography (left) and phase detection EFM (right) images of the surface of a thick-film resistor (TFR). EFM image depicts the conductive RuO₂ network (dark) exposed at the surface. 50µm scans.

Ferroelectric materials

Riportiamo a titolo di esempio l'immagine ricavata dalla scansione di un campione sulla cui superficie sono stati distribuiti dei domini ferroelectrici. L'area esaminata misura 2µm x 3µm, mentre i singoli domini misurano 500nm x 300nm [3].

Domini ferroelectrici depositati su un substrato isolante. E' indicata la polarizzazione normalizzata del campo in corrispondenza dei domini. La distanza tip-sample è stata di 60nm. L'area di scansione misura 2µm x 3µm.



Per materiali che non hanno una polarizzazione permanente vale l'analisi svolta precedentemente. La polarizzazione va calcolata auto-consistentemente; la risoluzione in ogni caso decresce con l'aumentare della separazione tip-sample, come messo in evidenza dalla seguente figura:

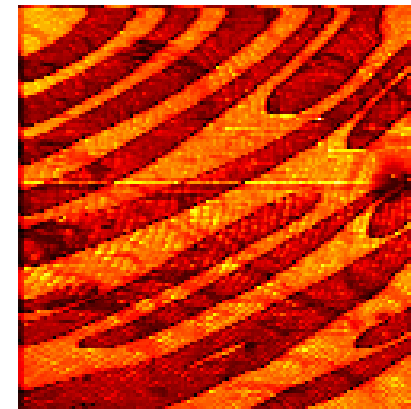


Image of ferroelectric domain structure in TGS sample by Voltage Modulation Atomic Force Microscopy
Scan size 27 µm x 27 µm

Conclusions

- ✓ AFM extends STM capabilities to *any kind* of material surfaces (not restricted to conductive as in STM)
- ✓ Topography can be retrieved with sub-nm accuracy by operation in either contact or non-contact modes
- ✓ Mechanical properties (e.g., hardness, Young modulus, etc.) can be measured at the local scale with nanoindentation techniques
- ✓ Lateral forces can be acquired and treated to get nanotribological information
- ✓ AFM “relatives” open the way to a wide variety of local measurements and imaging methods